Quaternary Science Reviews 24 (2005) 1159–1182

The role of seasonality in abrupt climate change

George H. Denton[a], Richard B. Alley[b,*], Gary C. Comer[c], Wallace S. Broecker[d]

[a]*Department of Earth Sciences and Climate Change Institute, University of Maine, Orono, ME 04469, USA*
[b]*Department of Geosciences and Earth and Environmental Systems Institute, Pennsylvania State University, University Park, PA 16802, USA*
[c]*GCI, Waukesha, WI 53186, USA*
[d]*Earth and Environmental Sciences, Lamont-Doherty Earth Observatory of Columbia University, Palisades, NY 10964, USA*

Received 21 July 2004; accepted 15 December 2004

Abstract

A case is made that seasonality switches dominated by wintertime were instrumental in abrupt climate changes in the North Atlantic region during the last glaciation and into the Holocene. The primary evidence comes from mismatches between mean annual temperatures from Greenland ice cores in comparison with snowline changes in East Greenland, northern Europe, and North America. The most likely explanation is a shutdown (or reduction in strength) of the conveyor. This allows the spread of winter sea ice across the North Atlantic, thus causing the northern region to experience much colder winters. Because they mimic the Greenland temperature rather than the snowline signal, changes in the Atlantic Intertropical Convergence Zone and the Asian monsoon may also share a winter linkage with Greenland. Thus the paleoclimate record is consistent with the notion that a huge continental sector of the Northern Hemisphere, stretching from Greenland to Asia, was close to an extreme winter threshold during much of the last glaciation. Winter climate crossed this threshold repeatedly, with marked changes in seasonality that may well have amplified and propagated a signal of abrupt change throughout the hemisphere and into the tropics.

1. The problem

The GISP2 ice core from Summit in central Greenland (Fig. 1) registers repeated abrupt changes in oxygen-isotope ratios during the last glaciation and into the early Holocene (Fig. 2) (Stuiver and Grootes, 2000). These isotope jumps reveal temperature (Severinghaus et al., 1998; Stuiver and Grootes, 2000). They occurred in years to decades. The rapid warmings amounted to as much as two thirds of the full glacial-interglacial amplitude. Switches in the continental-dust and sea-salt content of the atmosphere accompanied the rapid isotope changes (Mayewski et al., 1993, 1997). In whole or in part, the Greenland template of abrupt changes is now essentially replicated in North Atlantic sediment cores that reveal sea-surface temperatures (SSTs) (Bond et al., 1993) and in European lacustrine archives that preserve oxygen-isotope values of past precipitation (Grafenstein et al., 1999; Jones et al., 2002). Cariaco Basin sediment cores in the western tropical Atlantic show SST variations and shifts in the Atlantic Intertropical Convergence Zone (ITCZ) that were coeval with Greenland temperature changes within the dating errors (Hughen et al., 1996; Lea et al., 2003). Sediment cores from the Santa Barbara Basin on the California margin reveal surface- and intermediate-water fluctuations linked with abrupt reorganizations of atmospheric circulation over the North Pacific that appear correlative with the Greenland template (Hendy and Kennett, 1999). As measured in the Arabian Sea (Schulz et al., 1999; Altabet et al., 2002), the South China Sea (Kienast et al., 2001), and the Hulu Cave in China (Wang et al., 2001), the Indian and East Asian monsoons featured abrupt shifts in summer intensity that seem to match Greenland millennial-scale oscillations. Finally, the near-synchronous change of isotope ratios and methane

*Corresponding author. Tel.: +1 814 863 1700; fax: +1 814 863 7823.
E-mail address: ralley@essc.psu.edu (R.B. Alley).

0277-3791/$ - see front matter © 2005 Published by Elsevier Ltd.
doi:10.1016/j.quascirev.2004.12.002

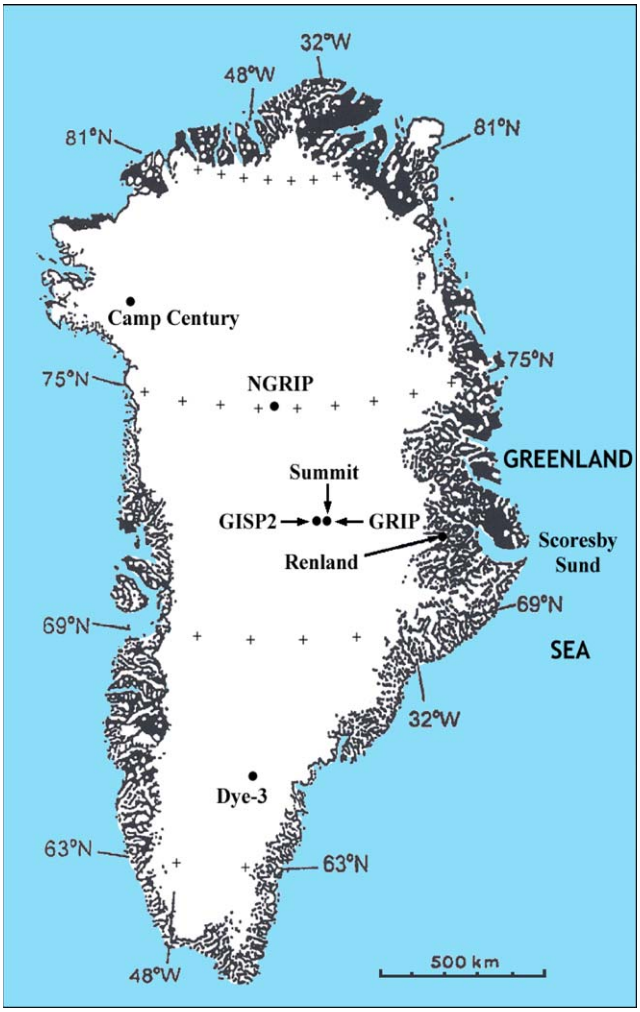

Fig. 1. Location of the Greenland ice cores. Adapted from Johnsen et al. (2001).

in the GISP2 ice core in Greenland indicates that the abrupt warming event at the end of the Younger Dryas likely involved the tropics (Severinghaus et al., 1998).

Thus the abrupt changes first recognized in Greenland more than 30 years ago (Dansgaard et al., 1971; Johnsen et al., 1972) are now known to have had an extensive geographic footprint in the Northern Hemisphere. Understanding these spectacular events is a pressing problem of paleoclimatology. In this paper we reinforce the hypothesis that the abrupt Greenland temperature changes are highly weighted toward the winter season. Our motivation comes from the examination of mismatches between ice-core temperature oscillations and moraine/snowline changes in East Greenland. In like manner, European paleotemperature records show evidence of extreme seasonality, for example, with very large cooling in winter compared to summer during the Younger Dryas (Atkinson et al., 1987; Isarin and Renssen, 1999). Moreover, the Asian monsoon featured drastic switches in seasonality, with the summer signal weakening and strengthening in lockstep with Greenland temperature, leaving winter monsoon circulation dominant during Greenland stades (Wang et al., 2001; Altabet et al., 2002). Therefore, seasonality seems to have been very important in abrupt climate switches. We postulate that severe winter changes were responsible for much of the amplitude of the jumps. If this argument has merit, any proposed explanation of widespread abrupt climate changes should accommodate a relatively muted summer signal along with a strong winter response, at least for the entire Greenland-North Atlantic region and probably for a large swath of Eurasia.

2. Greenland ice cores

Prominent in the GISP2 isotope record in Fig. 2 are the Dansgaard-Oeschger events between 26,000 and 60,000 years ago, along with the Bölling/Alleröd-Younger Dryas oscillation subsequent to the Last Glacial Maximum (LGM). Of particular importance to our discussion are the cold extremes of both the Younger Dryas and the Dansgaard-Oeschger events, which are equivalent to, or even colder than, those of the LGM. Also noteworthy is the fact that the warm peaks of the Dansgaard-Oeschger cycles reached nearly to interglacial values, whereas the warm Bölling peak actually achieved an interglacial level. Thus, the Dansgaard-Oeschger climate jumps ranged in amplitude from full-glacial to nearly full-interglacial conditions. The warming jump of several decades duration that initiated the Bölling was from slightly above full-glacial (Alley et al., 2002) to full-interglacial conditions.

Based on borehole paleothermometry, near-surface mean-annual air temperatures at Summit had a glacial-interglacial amplitude of 21–23 °C (Cuffey et al., 1995; Cuffey and Clow, 1997; Dahl-Jensen et al., 1998). This translates into an estimated borehole temperature calibration for oxygen-isotope ratios of 0.33‰ per degree for the glacial-interglacial difference (Cuffey et al., 1995; Dahl-Jensen et al., 1998). Because this is an average value, it does not constrain the exact relationship during abrupt climate changes. However, for the Bölling transition, isotopes of nitrogen and argon in trapped air in the GISP2 core yield a value of 9 ± 3 °C for warming of mean annual temperature over an interval of several decades, which gives a calibration for oxygen-isotope ratios of 0.38‰ per degree (Severinghaus and Brook, 1999). Both of these measurements show that the modern relationship of oxygen-isotope ratios and air temperature (0.67‰ per degree) cannot be applied to ice-age climate changes. Fig. 2 gives one solution to this problem by illustrating a calibration of the GISP2 isotope ratios to mean annual temperature on the basis of borehole paleothermometry (Cuffey and Clow, 1997). An implication of this calibration is that

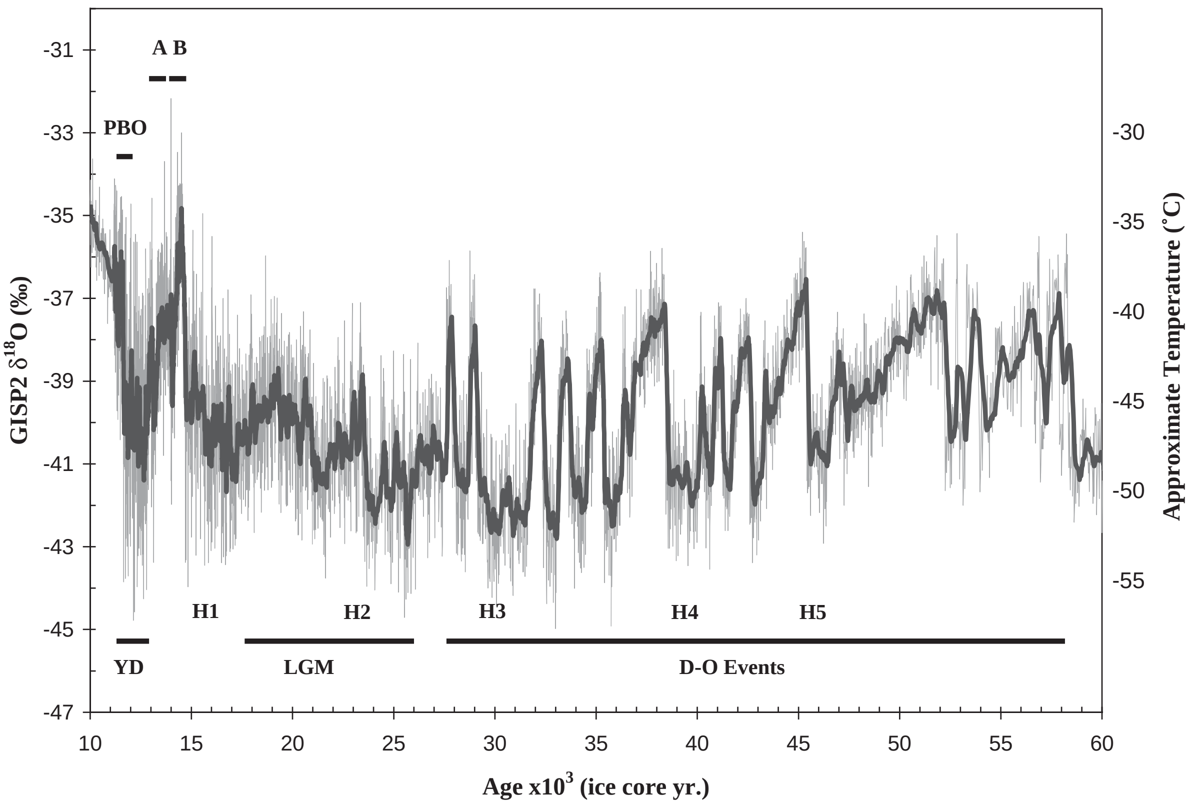

Fig. 2. The oxygen-isotope record from GISP2 taken from web site given in Stuiver and Grootes (2000). The isotope data are not smoothed. The temperature scale associated with the isotope shifts is adapted from Cuffey et al. (1994) and Cuffey and Clow (1997). B depicts the position of the Bölling, A is the Allerød, YD is the Younger Dryas, and PBO is the Preboreal oscillation. The LGM interval is chosen to correspond to the time when ice sheets and glaciers were at or near their maximum extents of the last glaciation, as shown in Figs. 9 and 10 and discussed in the text. D–O events refer to Dansgaard-Oeschger events. H1–H5 depict the positions of Heinrich events 1–5 transferred from North Atlantic sediment cores to the GISP2 isotope record. Each Heinrich event was marked by an outburst of Laurentide icebergs eastward across the North Atlantic. We follow the usage of Broecker and Denton (1989, p. 2481) whereby Dansgaard-Oeschger events "have durations on the order of a millennium and rise-and-fall times on the order of one century. In this regard they are akin to the Younger Dryas event." In GISP2 oxygen-isotope ratios (Stuiver, and Grootes, 2000), such events include a fast cold-to-warm transition, with the halfway mark reached as rapidly as two years and the culmination in 50 years. There then follows a long and slow temperature decline of between 400 and 4000 years duration, culminating in a sudden warm-to-cold transition that lasts about 80 years. The rapid cooling brings climate to a cold baseline that persisted until renewed abrupt warming. By an alternate usage not followed here, Dansgaard-Oeschger events are restricted to the abrupt cold-to-warm transitions embedded in the glacial-age $\delta^{18}O$ oscillations (Stuiver and Grootes, 2000).

mean annual air temperature at Summit during Younger Dryas cooling was about $-47\,^{\circ}C$, in close agreement with the value of $-46\pm3\,^{\circ}C$ ($15\pm3\,^{\circ}C$ colder than present) derived from analyses using the thermally fractionated gas trapped in ice (Severinghaus et al., 1998). Older abrupt switches also relate to temperature and have a calibration different from modern spatial changes (Landais et al., 2004)

As mentioned, the temperature-to-isotope ratio of 0.33–0.38‰ required for glacial time by the borehole temperature reconstruction and by isotopic fractionation of gases departs significantly from the theoretical (and observed) modern value of 0.67‰ per degree. A likely hypothesis to explain this difference is a marked increase in the seasonality of snowfall (Steig et al., 1994) at Summit during glacial times because of winter-time cooling and drying (Cuffey et al., 1995; Cuffey and Clow, 1997; Fawcett et al., 1997; Jouzel et al., 1997; Krinner et al., 1997; Alley, 2000; Werner et al., 2000, 2001). As an example of a physical basis for such proposed seasonality, Alley (2000) called for widespread freezing of North Atlantic surface water, thus curtailing wintertime heat flux from the Nordic Seas. Werner et al. (2000) postulated increased northerly advection over Summit of dry cold air masses during glacial winters.

The GISP2 and GRIP oxygen-isotope records from Summit in central Greenland are basically replicated in ice cores from Camp Century in northwestern Greenland, Dye 3 in southern Greenland, and north GRIP in northern Greenland, all located in Fig. 1 (Johnsen et al., 2001). Hence the climate signal in Fig. 2 appears to be robust throughout Greenland. Of particular importance to our further discussion of seasonality is the Renland core in East Greenland, taken from a plateau ice cap located about 400 km east of Summit on an isolated bedrock plateau just inland of Scoresby Sund (Fig. 1).

The oxygen-isotope ratios measured in the Renland ice core nearly match those from the inland GISP2 core at Summit. These similarities include full-glacial conditions at the cold extremes of Dansgaard-Oeschger events, a subdued LGM, a return to full-glacial conditions during the Younger Dryas cold reversal, and a prominent Preboreal oscillation. The location of such a core near the eastern edge of the ice sheet allows an alternate test, outlined below, of the hypothesis of enhanced Greenland seasonality during cold episodes.

3. Scoresby Sund moraine sequence

3.1. General statement

In August of 2003 we conducted a survey of the glacial geology of the Scoresby Sund and Kong Oscar Fjord region of East Greenland (Figs. 1 and 3). This survey included an aerial reconnaissance with flight lines totaling 10,000 km, complemented by examination of key areas on the ground. Our motivation came from the fact that only near Renland does a moraine sequence occur alongside a Greenland ice core. From comparison of these side-by-side records, we wished to explore the importance of seasonality in the Greenland temperature signal of abrupt climate change. Of particular significance to us were the Milne Land stade terrestrial moraines and their submarine equivalents of late-glacial age. During the course of our investigations of these moraines, we came to agree with the basic conclusions of Funder (1970, 1971, 1972a, b, 1978, 1989, 1990) and Funder et al. (1994, 1998), whose work is therefore referenced extensively below.

3.2. Scoresby Sund fjord region

Scoresby Sund and Hall Bredning basin (70–72°N) together form the most extensive embayment in the coastline of the Greenland Sea (Figs. 1 and 3). This embayment is broad, and barely reaches −600 m in its deepest part. Projecting far inland from the head of this embayment is a set of branching, steep-sided, narrow fjords. Nordvestfjord attains a record Northern Hemisphere depth of −1500 m (Funder, 1989). These branching fjords extend headward into a flattish, uplifted Tertiary erosion surface (Ahlmann, 1941a), isolating several bedrock remnants. Most of these remnants have largely retained their upper plateau surfaces, although one north of Nordvestfjord has been dissected into classic mountain glacial topography to form the Stauning Alper. Overall, the whole interconnected system of embayment and fjords penetrates 300 km inland from the mouth of Scoresby Sund on the Greenland Sea.

Major outlets from the ice sheet flow into the head of the fjord system, where they terminate in calving fronts. The isolated bedrock plateaus alongside the fjords are mantled with ice caps. One such local cap covers the Renland plateau. Another occurs on nearby Milne Land. Outlet glaciers from such plateau caps flow down into adjacent fjords. The Stauning Alper are now filled with alpine glaciers.

Scoresby Sund lies in the zone of continuous permafrost. Mean annual temperature close to sea level at the mouth of the sound is −8 °C (Funder, 1978).

3.3. Historical moraines

Three groups of moraines in the Scoresby Sund region are important for our discussion (Fig. 3). First, fresh moraines of so-called historical age occur 1–2 km beyond the snouts of all terrestrial ice lobes in the Scoresby Sund region and are associated with fresh trimlines (Funder, 1990) (Fig. 4A). Elsewhere in Greenland, most such moraines and trimlines are dated from historical records to the middle or late 19th century, although a few may have been deposited in the early 19th or middle 20th century (Ahlmann, 1941b, c, 1948, 1953; Weidick, 1959, 1963, 1968, 1972, 1994). Thus the historical moraines in the Scoresby Sund region almost certainly date to the Little Ice Age.

3.4. Milne Land stade moraines

An extensive terrestrial moraine system, named after Milne Land where it is well preserved, occurs near the inland margin of Scoresby Sund and Hall Bredning basin (Funder, 1970). This system features as many as 10 ridges forming a belt of lateral moraines about 5 km wide; the terminal positions were spread over as much as 20 km. These terrestrial moraines, among the largest in Greenland, have well-preserved constructional morphology. The outer boundary of the moraine belt is sharp, with a distinct weathering break (Funder, 1978, p. 25). Thus the system is taken to represent resurgence in late-glacial time. The terrestrial moraine belt has a submarine equivalent consisting of a major depocenter of acoustically laminated marine sediments that crosses the head of Hall Bredning basin (Dowdeswell et al., 1994).

The Milne Land stade moraines (Fig. 4B) and their equivalent marine deposits outline a former coalescent system of fjord, plateau, and alpine glaciers (Fig. 3). Greenland outlet glaciers, which still filled the fjords at the time of the Milne Land stade, extended a short distance out of the fjord mouths into western Scoresby Sund and Hall Bredning. At that time, outlet glaciers from the Renland plateau cap were tributaries to the Nordvestfjord and Øfjord ice tongues. Outlet glaciers from central and western portions of the plateau ice cap on Milne Land itself flowed into the main tongues in

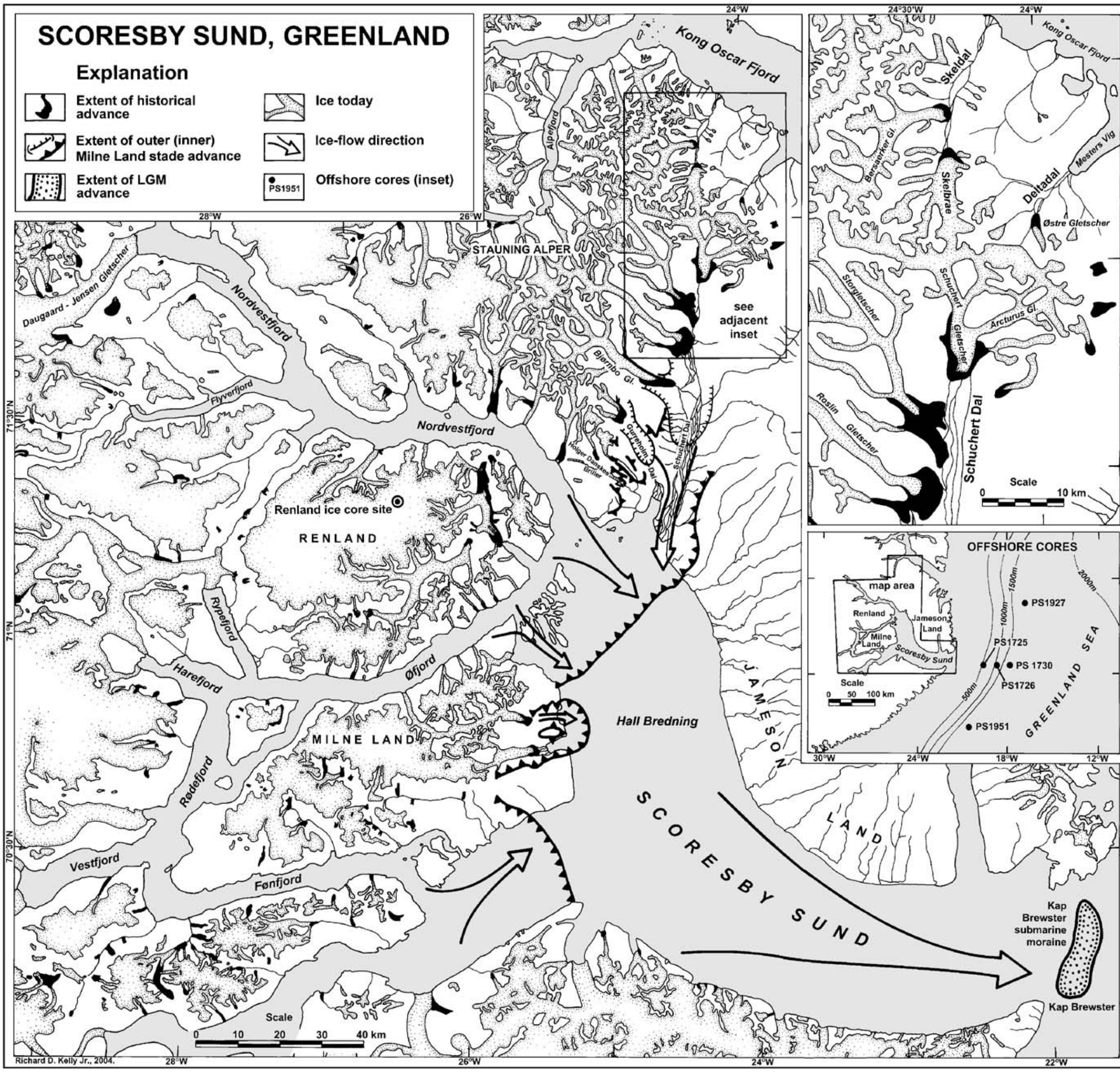

Fig. 3. Sketch map of former ice-marginal extents in Scoresby Sund, East Greenland. The positions of the historical (Little Ice Age) moraines are taken from Funder (1990) and from field observations. The approximate maximum extent of the Milne Land stade advance is taken from Funder (1978, 1990). The position of the ice margin where it crosses Scoresby Sund and the Hall Bredning basin is close to the major depocenter of laminated marine sediments (Dowdeswell et al., 1994). The position of the Kap Brewster submarine moraine is from Funder et al. (1996).

Øfjord and Fønfjord. However, the eastern outlets of the Milne Land cap remained independent, advancing only about 12 km beyond the so-called historic position of the Little Ice Age (Fig. 4B). Southward-flowing mountain glaciers of the Stauning Alper were tributary to the Nordvestfjord ice tongue. Eastward-flowing glaciers from the Stauning Alper coalesced in Schuchert Dal to form an ice tongue that extended southward along the valley axis to the head of Hall Bredning basin. Here the Schuchert Dal tongue barely coalesced with ice bulging southeastward out of Nordvestfjord (Funder, 1978, 1990).

Because of isostatic depression from ice loading, Milne Land stade glaciers terminated in a sea whose level was relatively higher than that of the present day. Thus terminal moraines are largely absent because glacier tongues were afloat. However, some lateral moraines descending from land can be tied to higher

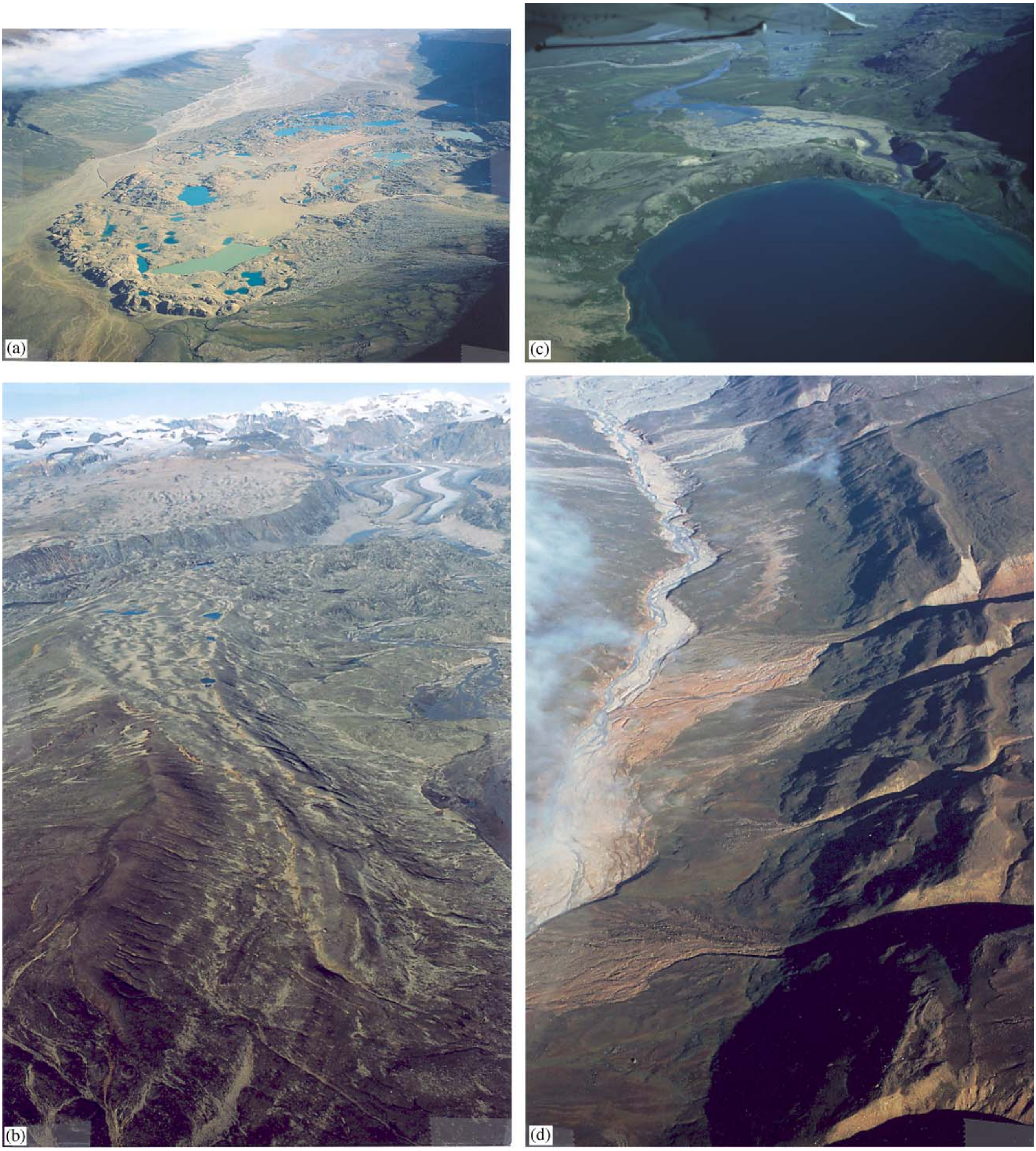

Fig. 4. Oblique aerial photographs of historical moraines and Milne Land stade moraines in the Scoresby Sund drainage. A shows historical moraine in front of Roslin Gletscher on the floor of northern Schuchert Dal. B shows the outer of the Milne Land stade moraines in eastern Milne Land, deposited by an eastern outlet glacier of the Milne Land plateau ice cap, visible in the background. The upper limit of the moraine swarm marks the maximum glacier extent during the Milne Land stade. At that maximum, the ice front was situated only 12 km seaward of the light-colored historical moraine (Funder, 1978) visible in the background. C shows the inner Milne Land stade moraine (and associated outwash delta) that dammed the eastern end of a lake in the valley Holger Danskes Briller (Fig. 3). This moraine probably dates to the Preboreal oscillation. D depicts the left lateral moraine deposited in Gurreholm Dal during the late phase of the Milne Land stade. We take this moraine to represent a glacier readvance. Gurreholm Dal is a tributary that joins Schuchert Dal near Hall Bredning. The glaciers that deposited this lateral complex originated in the Stauning Alper. In the background is the outer edge of the historical moraine (light colored) deposited by this glacier complex at head of Gurreholm Dal.

relative sea levels because they grade into marine embankments, have associated outwash deltas, or intersect raised beaches. In eastern Milne Land itself raised shorelines truncate the outermost moraines at 120 m elevation; in southern Milne Land a marine cliff at 135 m elevation is cut into the oldest deposits (Funder, 1978, p. 25). The inner Milne Land stade moraines are associated with lower relative sea levels.

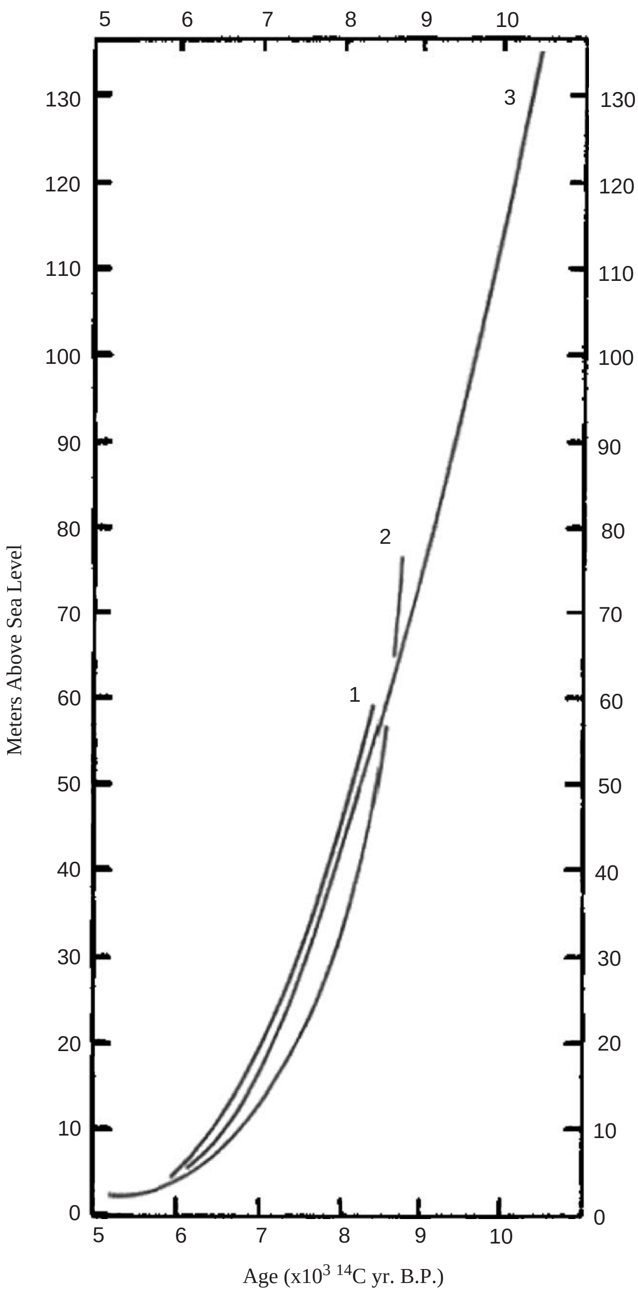

Fig. 5. Uplift curves for East Greenland middle fjord district. Curve 1 is from Mesters Vig (Washburn and Stuiver, 1962; Washburn, 1965). Curve 2 is from Skeldal (Lasca, 1969). Curve 3 is from western Scoresby Sund and Hall Bredning (Funder, 1978). See Fig. 3 for locations. Adapted from Funder (1978).

The geomorphic relation between moraines and raised shorelines affords a method to radiocarbon date glacier resurgence during the Milne Land stade. Fig. 5 depicts the three uplift curves useful for this purpose. The two most completely dated of these curves come not from the Scoresby drainage, but from Mesters Vig (Washburn and Stuiver, 1962; Washburn, 1965) and Skeldal (Lasca, 1969), both situated on the south flank of Kong Oscar Fjord about 40 km north of the head of Schuchert Dal (Fig. 3). Expanded alpine glaciers from the Stauning Alper flowed into all three of these valleys (Schuchert Dal, Skeldal, and Mesters Vig), and hence each should have experienced the same glacial history.

Uplift curve 1 in Fig. 5 from Mesters Vig is based on 20 radiocarbon control points (Washburn and Stuiver, 1962). The oldest date is 8780 ^{14}C yr BP from shells at 59–69 m elevation. Uplift curve 2 in Fig. 5 from Skeldal is calibrated on 14 radiocarbon dates of shells from raised marine deposits. All the shell sites lie within the limits of the last readvance of alpine ice through Skeldal. The oldest shell came from about 60 m elevation and dates to 8955 ^{14}C yr BP (Lasca, 1969). Uplift curves 1 and 2 are quite similar, except for the possible "false steepening" effect for Mesters Vig discussed below. Both register unloading of glacier ice from Skeldal and Mesters Vig in early Holocene time.

Because they rest on the valley floor at only 60–76 m elevation, the oldest shell samples from Skeldal and Mesters Vig (Fig. 5) simply afford minimum limiting ages for the last through-valley glacial advance. Therefore, uplift in western Scoresby Sund itself must be used to date the Milne Land stade moraines. In this regard, Funder (1978) constructed uplift curve 3 in Fig. 5 for the area of the Milne Land stade moraines in western Scoresby Sund and Hall Bredning basin. Unlike the tightly constrained sampling areas for Mesters Vig and Skeldal, however, the control points for the Scoresby curve 3 come from a zone 160 km long, stretching from Schuchert Dal to southern Milne Land. Such an extensive spread of data points is thought to be justified because the sampling zone follows the limit of the Milne Land stade moraines, and hence is taken to have suffered the same isostatic history. The age of the upper limit for the Mesters Vig and Skeldal curves is controlled by radiocarbon dates of shells. But note that for the Scoresby curve, the age of the local marine limit is extrapolated upward to 135 m from the oldest control point at 107 m dated to 9750 ^{14}C yr BP in the mouth of Schuchert Dal.

The three uplift curves in Fig. 5 are in general agreement. The only discrepancy is the steeper older limb of the Mesters Vig compared to the other two curves. Funder (1978) suggested that the Mesters Vig curve suffers from the phenomenon of "false steepening". With curves based on shell samples such as those at Mesters Vig, as opposed to curves based on driftwood buried in raised beaches, a common difficulty is selecting the sea level tied to each shell sample. Potential errors involved with such selections become greater with increasing distance from the local marine limit. This may result in old samples being tied to sea levels that are too low, producing a falsely steep older portion of the uplift curve.

By reference to emergence curve 3 in Fig. 5, Funder (1978, p. 25) placed the age of the outermost moraines in Milne Land at 10,100–10,400 ^{14}C yr BP, that is, within the Younger Dryas. The inner moraines graded to lower relative sea levels were placed in early Preboreal time. The best dated of the innermost moraines is that which dams the eastern end of a lake in the valley Holger Danskes Briller near the mouth of Schuchert Dal (Fig. 4C). A component of this moraine is an outwash delta graded to a former sea level at 101 m elevation. A shell sample corresponding to this level a few kilometers to the east afforded an age of 9740 ^{14}C yr BP (Funder, 1978). Hence the innermost Milne Land stade moraine probably dates to the Preboreal oscillation (see Fig. 2 for timing).

Shells dated at 8520 and 7750 ^{14}C yr BP from two sites that have not been overrun occur on the floor of Schuchert Dal within 2.5–5 km of the historical moraines of Roslin Gletscher (Street, 1977; Funder, 1978). In neither case is there an obvious ridge between the shell sites and the historical moraine. Further, the distribution of marine terraces on both sides of the valley precludes advance of the local valley glaciers in Schuchert Dal beyond their historical limits since 8520 ^{14}C yr BP (Street, 1977).

The distribution of radiocarbon-dated shells in or near Schuchert Dal suggests that retreat from the inner Milne Land stade moraines began after 9750 ^{14}C yr BP and was completed prior to 8520 ^{14}C yr BP, when Schuchert Dal glaciers had retreated at least to the position of the local historical moraines. That a similar situation occurred in Skeldal and Mesters Vig is shown by radiocarbon dates of marine shells from sites that have not been overrun and that are close to historical moraines. Shells dated to 8650 ^{14}C yr BP in Skeldal are situated 5 km from the historical moraines of Beraerkerbre (Lasca, 1969). In Mesters Vig, shells dated to 8480 ^{14}C yr BP occur within 3 km of the historic moraines of Østre Gletscher (Washburn and Stuiver, 1962). In neither of these cases is there an obvious moraine ridge between the shell sites and the historical moraines.

Several weaknesses exist in the chronology of the Milne Land stade moraines, as currently understood. First, ages have been assigned to the outer moraines by extrapolation rather than direct dating of uplift curve 3 in Fig. 5. Second, the terminal retreat that would be expected from a moraine belt of Younger Dryas age has not been recognized. Instead deglaciation of Schuchert Dal, for example, did not begin until after 9750 ^{14}C BP One possible reason for this lack of terminal Younger Dryas recession is that readvance of Schuchert Dal glaciers during the Preboreal oscillation reached all the way to the inner Milne Land stade moraine ridge. We favor this explanation because the inner ridge is sharp and morphologically distinct from the older Milne Land stade moraines. An example of this inner sharp ridge is given in Fig. 4D. The lack of evidence for terminal Younger Dryas recession could also be explained if all the moraine ridges were deposited during the Preboreal oscillation (Funder and Hansen, 1996; Björck et al., 1997), with subsequent retreat from the moraine belt.

The following comparison of Greenland moraine and ice-core records is based on the working hypothesis that the Milne Land stade moraines represent ice margins dating to both the Younger Dryas and the Preboreal oscillation. Final resolution of the matter will require radiocarbon dates of shells from near the marine limit, along with exposure dates from the moraines themselves. If such dates should show that all Milne Land stade ridges date from the Preboreal oscillation, then the Younger Dryas ice margin must have been located behind the outer limit of the Milne Land stade moraine belt. In that case the seasonality of Younger Dryas climate would have been even more pronounced than argued below.

3.5. *LGM ice margin*

At the LGM, the major fjord outlet glaciers coalesced with expanded plateau ice caps and Stauning alpine glaciers to feed an enormous grounded ice tongue that extended seaward to the mouth of Scoresby Sund (Fig. 3). Here the main LGM position of the calving terminus appears to be marked by the Kap Brewster submarine moraine (Dowdeswell et al., 1994; Mangerud and Funder, 1994), although it is possible that the LGM grounding line at times extended beyond the Kap Brewster moraine and onto the inner continental shelf (Funder et al., 1998). Along its lateral margins, the LGM ice tongue was bounded by land, reaching surface elevations of 200–400 m on the south side of Scoresby Sund inland of Kap Brewster (Mangerud and Funder, 1994). On the north side of the sound, the lateral margin appears to have been quite low on southern Jameson Land (Veranger et al., 1994). The timing of LGM maxima is registered in radiocarbon-dated pulses of ice-rafted debris (IRD) in marine sediment cores taken seaward of the mouth of Scoresby Sund (Figs. 3 and 6). As can be seen in Fig. 6, there is a concentration of IRD between 21,000 and 13,000 ^{14}C yr BP, with a subsidiary peak between 26,000 and 29,000 ^{14}C yr BP. The interpretation given by Funder et al. (1998) in the right-hand column of Fig. 6 calls for ice expansion

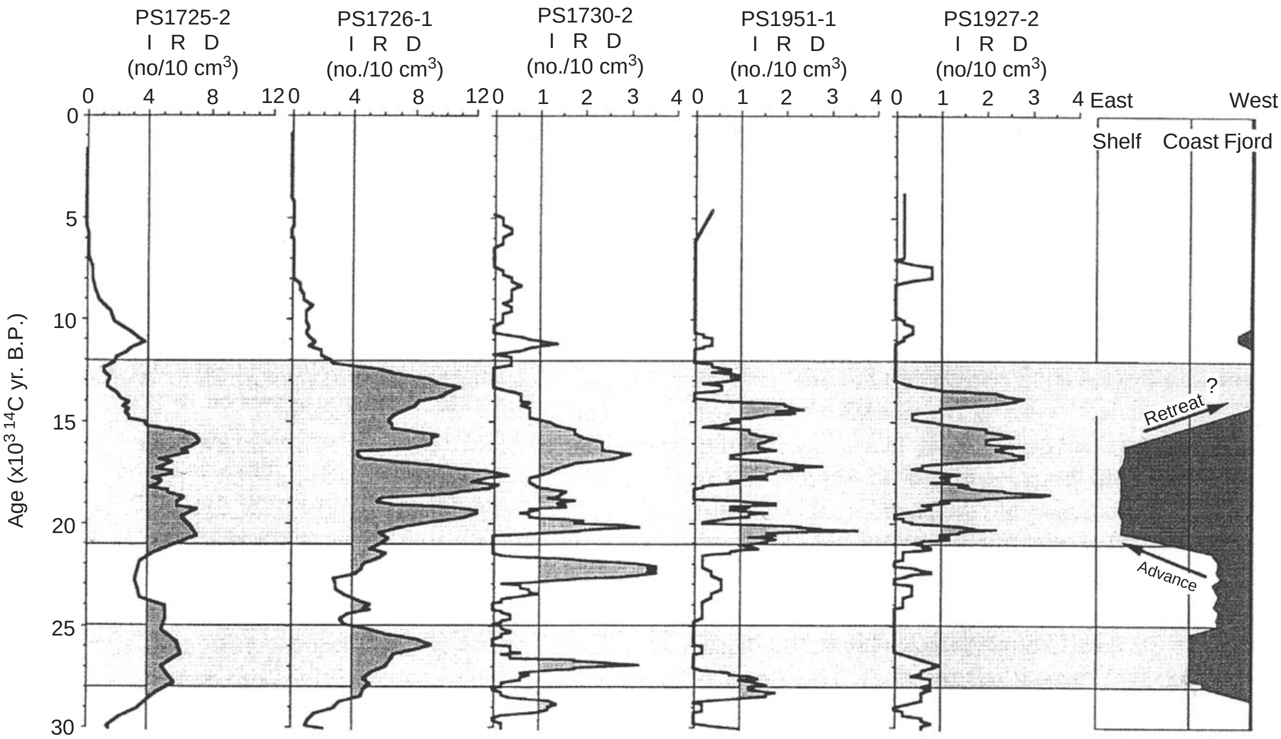

Fig. 6. Composite diagram of pulses of ice-rafted debris in marine sediment cores off the mouth of Scoresby Sund, plotted against a marine-reservoir-corrected radiocarbon age scale. The diagram is based on data in Stein et al. (1996) and Nam et al. (1995). The interpretation of ice-rafted sediment pulses in terms of ice-front fluctuations in Scoresby Sund is given in the right-hand column. Adapted from Funder et al. (1998).

across the present-day coast onto the continental shelf during the LGM between 21,000 and 13,000 ^{14}C yr BP.

4. East Greenland moraines and ice cores compared

4.1. Snowlines

Moraine sequences such as those in East Greenland register length changes of glaciers that are tied to variations in equilibrium-line altitudes (ELAs). In turn, ELA changes are linked to glacier mass balance controlled by the relation of summer ablation to winter precipitation. It has long been recognized that mean ablation-season temperature is closely correlated to the amount of ablation (Ahlmann, 1924; Liestøl, 1967). The line of reasoning given in this paper is based on the premise that glacier length and ELA are controlled primarily by temperature during the ablation season.

Snowline variation is a widely used paleoclimate indicator. The snowline is conventionally taken as the divider between snow-covered and snow-absent regions of a glacier at the end of the melt season (typically August in the Northern Hemisphere). Usually snowline is not far from the equilibrium line that separates the zones of net mass accumulation and loss on the glacier surface (e.g., Oerlemans, 2001). An empirical relation (with much physical basis) shows that about 60% of the surface of a steady glacier ending on land will be in the accumulation zone and 40% in the ablation zone. This relation allows reconstruction of ELAs by the accumulation-area-ratio (AAR) method from surface contouring of former glaciers reconstructed from moraines and trimlines (e.g., Porter, 1975). Application of the atmospheric lapse rate to elevation changes of the snowline, with corrections if possible for winter precipitation and isostasy, is then used for summer paleothermometry.

The utility of glacier extent or snowline elevation as a paleothermometer is illustrated by research such as that of Oerlemans (1994), who found that the dominant summer temperature control on glacier mass balance allowed an estimation of 20th century warming (from glacier changes) that closely resembles instrumental measurements. Oerlemans (2001, p.128) summarized a study by the European Ice Sheet Modeling Initiative and found that, for a range of mountain glaciers and ice caps, "The melting of ice due to climatic warming is not easily compensated for by an increase in precipitation. For most glaciers the increase in precipitation needed to cancel the effect of a 1 °C-warming is 30–40%". A survey of additional publications indicates that an even higher accumulation-rate increase of 40–50% is needed to offset the effects of a 1 °C warming on some land-ending glaciers (Alley, 2003). In comparison, the increase in saturation vapor pressure with a 1 °C warming is only about 7%, entirely insufficient to offset the effects of increased summer temperature on melting even if allowance is not made for the switch of some precipitation from snow to rain.

The dominance of summer temperature change over other climatic factors may be understood intuitively. The surface of a melting glacier remains at 0 °C, with heat transfer primarily by sensible heat and net radiation. Because of the very high albedo of dry snow compared to wet snow, and of wet snow compared to ice, the onset of melting roughly doubles the absorbed radiation, and the switch from wet snow to bare ice roughly redoubles the absorbed radiation (e.g., Paterson, 1994), so warming can cause a factor-of-two-or-larger increase in absorbed radiation over important parts of a glacier. Sensible heat transfer increases with the temperature difference between the 0 °C surface ice and the near-surface air. For a region with, say, 1 °C air temperature, a 1 °C warming will double the heat transfer. Hence, by removing snow and increasing air temperature over melting ice, even a small warming can greatly increase mass loss by melt. In comparison, effecting two-times changes from other parts of the climate system (e.g., windiness, precipitation, cloudiness) is not nearly so easy, and is not expected to be coupled with offsetting summer temperature changes. Incorporating such considerations into physical models yields the qualitative and quantitative results summarized above, with glaciers usually more sensitive to melt-season temperature than changes in other climatic factors (e.g., Oerlemans, 2001).

We thus presume that glacier length and snowline variations are driven largely by changes in the mean melt-season temperature. However, it is unequivocally true that glaciers are also affected by many other climatic and glaciologic factors, including wind speed, cloud cover, relative humidity, precipitation, debris cover, glacier surging, kinematic waves, and changes in basal sliding and till deformation. However, the sensitivity of the mass balance of glaciers to summer temperature change is very much higher than the sensitivity to other climatic factors. Moreover, dynamic glaciological changes such as surges commonly average out over years or decades so that even those glaciers in which such changes occur can be used for reconstructing climatic conditions that were stable for at least decades. Therefore, variations of glaciers ending on land, averaged across ice-flow perturbations such as surges, are primarily caused by summer temperature changes.

Glaciers that calve icebergs, on the other hand, do not balance snow accumulation entirely by surface melting. The behavior of tidewater glaciers is thus linked to calving dynamics as well as to climate. As a consequence, such complex glaciers can exhibit seemingly anomalous behavior. Even so, Weidick (1959, 1994) noted that over the period of historical observation the tidewater glaciers of southern and western Greenland generally exhibited behavior similar to that of nearby landlocked glaciers. It should also be noted that tidewater glaciers recorded the Younger Dryas cold reversal along the southern and western coast of Norway (Andersen, 1981).

We note that although change in glacier extent primarily reflects variation in summertime temperatures, glaciers do not distinguish between maximum melt-season temperature and melt-season duration. Glaciers instead respond to the integrated temperature above freezing, which usually is expressed as degree-days (one day at 10 °C and ten days at 1 °C have approximately the same effect on glacier melting; e.g., Oerlemans, 2001).

4.2. Greenland seasonality

Paleothermometry in the GISP2 and GRIP boreholes indicates about a 1 °C mean annual temperature lowering during the Little Ice Age (Alley and Koci, 1990; Cuffey et al., 1994; Dahl-Jensen et al., 1998), a value commensurate with the position of the Little Ice Age historical moraines close to present-day glacier termini in the Scoresby Sund region (Fig. 3). But the mean-annual-temperature lowering relative to today measured in the GISP2 ice core for Younger Dryas time is about 15 °C (Severinghaus et al., 1998), or 15 times the Little Ice Age value. This very large difference in mean-annual-temperature depression between the Little Ice Age and the Younger Dryas raises the question as to whether ELA lowering responsible for glacier expansion during the Milne Land stade was compatible with a change in summer temperature that was this dramatic.

In contrast to gas-fractionation paleothermometry in ice cores, which shows a return to nearly full-glacial conditions in Younger Dryas time, glacier expansion during the Milne Land stade fell well short of the LGM ice-marginal position at or beyond the seaward mouth of Scoresby Sund. In other words, glaciers were much shorter during the Milne Land stade than they were at the LGM (Fig. 3). In fact, in eastern Milne Land independent outlet glaciers of the plateau ice cap extended only about 12 km beyond the historic Little Ice Age moraines (Figs. 3 and 4). Such restricted glacial expansion is consistent with the muted late glacial ice-rafting pulse compared to those of the LGM in marine sediment cores taken seaward of Scoresby Sund (Fig. 6).

Viewed in another way, if the 15 °C cooling during the Younger Dryas were evenly distributed between summer and winter, snowlines would have depressed more than 2000 m in Renland, Milne Land, and the Stauning Alper, even with corrections for isostatic depression and for reduction in winter precipitation. This means that snowlines, which now vary from 1200 to 1500 m elevation, would have been depressed hundreds of meters below sea level if that were, in fact, possible. Whether such dramatic snowline depression actually occurred can be tested easily. Because of the flow vectors within a glacier, lateral moraines such as those deposited during the Milne Land stade form only alongside the ablation zones of glacier tongues, and hence occur at lower elevations than the coeval ELA. Thus minimum elevations of former ELAs are given by the upper limit of lateral moraines (Andersen, 1954, 1968).

That snowlines were not depressed nearly as much as would be implied by ice-core thermometry can be shown by the position of well-preserved Milne Land stade lateral moraines well above sea level. One example comes from the flattish terrain of eastern Milne Land (Figs. 3 and 4). Here the outer lateral moraines of the Milne Land stade rise inland from near the coast to about 550–600 m elevation alongside outlet glaciers that drain a small upland ice cap. This elevation represents a lower limit for the Milne Land stade snowline, because steep valley walls, as well as the former merger of outlet and low-elevation plateau ice caps, preclude the existence of the moraines at higher elevations. As present-day snowline in eastern Milne Land is about 1200 m, snowline lowering during the Milne Land stade was at most 600–650 m. About 100 m must be added to account for isostatic depression. Even taking into account a possible 50% reduction of winter precipitation, this means that mean summer temperature depression during formation of the outer Milne Land stade moraines was no more than 5.5 °C lower than today's value.

A second example comes from Gurreholm Dal, a tributary of Schuchert Dal alongside the Stauning Alper (Fig. 3). Near the valley mouth, the outermost Milne Land stade lateral moraines extend to at least 450 m elevation. A prominent inner Milne Land lateral moraine shown in Fig. 4D reaches to 750 m elevation on the north wall of upper Gurreholm Dal. This lateral was deposited by coalesced alpine glaciers flowing southeastward from the Stauning Alper down the axis of Gurreholm Dal. Present-day snowline on these glaciers is close to 1200 m. Thus compared to today's value, snowline dropped 450 (inner moraine) to 750 (outer moraine) during the Milne Land stade. Following the procedures of Dahl and Nesje (1992), another 100 m must be added to this value to compensate for the isostatic depression illustrated in Fig. 5. Taking into account a possible decline of 50% in precipitation, the mean summer ablation-season temperature was about 4.3 °C (inner moraines) to 6.1 °C (outer ridges depicted in Fig. 4B) below today's value.

It is evident that glacier lengths and snowline depressions during the Milne Land stade both show major mismatches with the Greenland ice-core records, including that of the Renland core adjacent to western Scoresby Sund. To us, the most plausible explanation involves seasonality. The mismatch can be accommodated if a large fraction of the ice-core temperature lowering of 15 °C below today's values during the Younger Dryas occurred in the winter season. For example, if summer temperature decline measured from snowline lowering associated with the outer moraines is 5.5–6.1 °C, then the winter depression for the coldest month must have been about 24 °C in order to account for a mean annual temperature of 15 °C below today's value. Thus a primary reason for the huge difference between the Little Ice Age and the Younger Dryas temperature depression measured in ice cores can be traced to dramatic changes in the temperature of the winter season, accompanied by much smaller changes in summer temperature. With regard to this interpretation of the record, we note that cooling over snow on the surface of the Greenland Ice Sheet is commonly amplified by development or strengthening of surface-temperature inversions, such that the temperature change at the surface is larger than that in the mean troposphere (e.g., Cuffey et al., 1995); this effect may have contributed to wintertime cooling on ice sheets. However, the near-surface amplification of cooling was probably not particularly large (Cuffey et al., 1995; Werner et al., 2001).

We mention in passing that a situation similar to that of the Younger Dryas occurs with regard to the prominent 8200-year cold event in the GISP2 core, calculated as 5 °C from gas isotopic fractionation (Kobashi et al., 2003), consistent with the estimate by Alley et al. (1997) of 6 °C by applying the calibration of 0.33‰ (Cuffey et al., 1995) to the oxygen-isotope jump of 2‰ from the early Holocene baseline value. The position close to the so-called historical moraines in Schuchert Dal, Skedal, and Mesters Vig of sample sites for shells that produced radiocarbon dates of 8650–8480 ^{14}C yr BP severely limits the magnitude of glacier advance at 8200 years ago (~7500 ^{14}C yr BP). The lack of obvious moraines between the shell sites and the historical ice-frontal positions suggests that any frontal advances during the 8200-year event did not exceed those of the Little Ice Age. Again, a likely explanation is seasonality, with most cooling in the winter.

The conclusion about extreme seasonality carries with it the implication that a large fraction of the abrupt temperature switches that both initiated and terminated the Younger Dryas cold pulse in Greenland occurred in the winter season. In one sense, these and other similar such events repeated throughout the Greenland ice-core records can be viewed as abrupt switches in seasonality, with winter changes dominant. Such an inference about extreme Greenland seasonality switches is consistent with the observation from a late-glacial lacustrine record that Younger Dryas summers in southern Greenland were anomalously warm while at the same time winters were cold (Björck et al., 2002). It is also in accord with the inferences of seasonality derived from the ice cores themselves, as discussed earlier.

5. European seasonality

We now address the question of whether the extreme seasonality shifts associated with abrupt climate switches in Greenland were a widespread phenomenon or whether they were only regional. We start by exploring the Younger Dryas event in Europe. We then move to a discussion of older mismatches between ice-core and moraine signals.

The oxygen-isotope records of lacustrine carbonate or ostracods from the British Isles (Jones et al., 2002) to middle Europe (Grafenstein et al., 1999; Eicher and Siegenthaler, 1976) show remarkable similarities with Greenland oxygen-isotope ratios through the past 15,000 years. In both cases abrupt climate events impacted the Bölling and the Younger Dryas. The question is whether the same extreme seasonality changes inferred for Greenland also characterized these abrupt events in Europe.

Beetle fossils allow reconstruction of late-glacial winter and summer temperature changes for the British Isles (Atkinson et al., 1987). The results are based on the climate tolerances of 350 carnivorous species of beetles. They come from 57 faunas collected at 26 sites. Full pleniglacial conditions persisted right up to an abrupt transition to nearly full interglacial conditions at the beginning of the Bölling. Just before this transition the coldest winter months were between −20 and −25 °C, and the climate was continental with a range between the warmest and coldest months of 30–35 °C, more than double today's value. The Bölling transition involved 7–8 °C warming of summer temperature and about 25 °C warming of winter temperature of the coldest month. At the Bölling peak, summer warmth reached 17 °C and the coldest winter month was 0–1 °C; such conditions are comparable to those of today, although slightly more continental. At the peak of the subsequent Younger Dryas cold reversal, mean annual temperatures were about 15 °C below today's value. The coldest winter month may have dropped to −25 °C and summer to 10 °C. Thus the climate again became continental, with the largest change occurring in winter.

The climate-indicator-plant-species method has been used to determine the minimum (lowest) July temperature that would have been possible for northern and central Europe during the Younger Dryas cold reversal (Isarin and Bohncke, 1997). The method rests on the relationship between plant distribution and temperature (Iversen, 1944). The idea is that individual species of plants and trees require a minimum summer temperature for flowering and reproduction. Thus a list of indicator species, each tagged with the minimum mean July temperature necessary for reproduction, was used for temperature reconstruction. Particular attention was focused on the themophilous plant *Typha latifolia*, an important indicator for high July temperatures (Iversen, 1954). A potential problem that must be dealt with carefully in such studies is that plant distribution can be influenced by factors other than temperature. To reduce this problem, Isarin and Bohncke (1997) used a database of as many as 140 late-glacial pollen and plant macrofossil diagrams. The results show relatively modest summer cooling, even for the severe first half of the Younger Dryas. The July values for the British Isles indicate a lowering of about 3 °C compared to today. July temperature lowering was about 4–5 °C across much of northern and central Europe, with the largest decline of about 6 °C just south of the Scandinavian Ice Sheet in Sweden.

Chironimid-inferred Younger Dryas mean July air temperatures give comparable values to the plant indicator species method. Compared to today's values, July cooling in the severe early part of the Younger Dryas amounted to about 5 °C at Whitrig Bog in southeast Scotland (Brooks et al., 1997; Brooks and Birks, 2001), and slightly more than 5 °C at Kråkenes Lake in western Norway (Brooks and Birks, 2001).

Lowering of glacier equilibrium line determined from Younger Dryas moraines, compared to today's values, amounted to about 350 m in the European Alps (Maisch, 1982, 1987, 1992). Farther north in the British Isles, Younger Dryas cirque glaciers developed in Ireland and Wales; cirque and valley glaciers in the Lake District, and extensive plateau icefields, outlet glaciers, and cirque glaciers in the western Scottish Highlands (Sissons and Sutherland, 1976; Sissons, 1979a, b; Sutherland, 1984; McDougall, 2001). Regional firn-limit altitudes were lowered to as little as 300 m on the southwestern edge of the highlands, rising north-eastward to about 800 m in the highlands (Sissons, 1979b).

In western Norway, the value for Younger Dryas ELA depression below the modern level, determined from moraine ridges, was about 450 m in the inner sector of Nordfjord (Fareth, 1987). In the western Nordfjord area near the coast of the Norwegian Sea, the average ELA lowering of 14 glaciers reconstructed from moraines was about 600 m compared to the present-day steady-state ELA (Larsen et al., 1984). Other values for comparable lowering are 475 m in northern Norway (Andersen, 1968), 400 m in the Hardangerfjord area south of Bergen (Follestad, 1972), 350–400 m just south of Hardangerfjord (Anundsen, 1972), and 450–600 m in southern Norway (Andersen, 1954).

Using the AAR method, and taking into account both isostatic depression and reduced winter precipitation, Dahl and Nesje (1992) computed a mean ablation-season (summer) temperature depression, compared to today, of $4.3 \pm 0.3\,^{\circ}\mathrm{C}$ from Younger Dryas ELA depression in inner Nordfjord, western Norway. A different procedure applied to Scotland (Sissons and Sutherland, 1976; Sissons, 1980) and the outer Nordfjord area (Larsen et al., 1984) produced a larger value for temperature depression. This alternative involves estimating the accumulation at the reconstructed former ELA, and then noting the associated temperature for the same accumulation value from a temperature-accumulation graph at the ELA constructed for modern Norwegian glaciers and given by Liestøl (1967), Sutherland (1984), and Sissons (1979a). Thus this method depends on making estimates of Younger Dryas precipitation, which are required in calculations of summer temperature values from lower ELAs. Isarin and Bohncke (1997) suggested that the resulting temperature calculations may be incorrect, simply because reliable estimates of Younger Dryas precipitation do not exist.

Overall, a consistent picture emerges of summer temperature decline during the Younger Dryas for northern and central Europe, despite the modest discrepancies among the relevant paleoclimatic indicators. After evaluating all available data and uncertainties, Isarin and Renssen (1999) concluded that summer temperatures in Europe, adjusted to sea level, ranged from 8 °C in the north to 13 °C in the south and east. These values are 3–7 °C below those of today.

In contrast to these relatively modest values for depression of European summer temperatures in the Younger Dryas, mean annual temperatures declined 12–17 °C below today's values (Fig. 2 in Isarin et al., 1998), with winter temperatures of the coldest month plunging on average about 22 °C (Fig. 3 in Isarin et al., 1998), as northern Europe reverted to a perglacial environment (Ballantyne and Harris, 1994). Thus, the extreme coldness of the Younger Dryas, and the common notion that conditions returned to full-glacial values, is due largely to this sharp decline in winter temperature. It has been further noted that the modern winter climate gradient inland across northern Europe vanished during the Younger Dryas. Instead, extreme continentality, with very cold winters, extended uniformly from the Atlantic seaboard inland at least to Poland (Isarin et al., 1998). The annual temperature range for the entire area of northern and central Europe is placed at 30–34 °C (the difference between the mean January and July estimates); this represents an increase compared to the present day of 20 °C for the British Isles and Ireland, with smaller increases inland (Isarin et al., 1998; Isarin and Renssen, 1999).

The evidence for the severe mean annual temperature drop in Europe during the Younger Dryas is derived largely from widespread periglacial features, although the overall conclusions compare well with those from the beetle data discussed above. A mean annual temperature threshold of −8 °C comes from the distribution of fossil ice-wedge polygons in coarse-grained substrate (Isarin et al., 1998; Isarin and Renssen, 1999). A threshold of −4 °C comes from the distribution of mineral palsas, open-system pingos, ice-wedge polygons in fine-grained substrate, and large cryoturbations. A threshold of −1 °C is placed at the boundary between discontinuous permafrost and seasonal frost. From the reconstruction of isotherms based on these features, the mean annual temperature north of 54°N is placed below −8 °C; that of the region between 51 and 54°N is placed below −4 °C; and that between 50 and 51°N is placed below −1 °C (Isarin and Renssen, 1999). Once the mean annual isotherms are established from periglacial features, the mean temperature of the coldest month for any particular locality is calculated from the mean July and the mean annual temperatures (Isarin et al., 1998). It is important to note that wind-direction indicators continued to show westerly flow during this interval, and so the extreme cold was not the result of a shift in atmospheric circulation that imported Siberian air from the east (Isarin et al., 1997, 1998).

From this comparison of biologic and periglacial proxies, it appears that the same extreme seasonality switches that marked abrupt Younger Dryas climate changes in Greenland also occurred in northern and central Europe. This picture is consistent with a reconstruction of late-glacial climate changes in central Europe from Meerfelder Maar and tree-ring archives. The implication is that the Younger Dryas cooling was principally a winter phenomenon, with no substantial summer change at all except in the length of the growing season (Lücke and Braver, 2004; Friedrich et al., 2004). It is also consistent with the differences in the Younger Dryas moraine and ice-core signals. In Fig. 2, the Younger Dryas cold reversal represents a return to full-glacial conditions. But such a situation does not pertain to moraine extent and snowline lowering in Europe. By the end of the Alleröd, the Scandinavian Ice Sheet had shrunk to about half of its LGM extent (Andersen, 1981). The ice cover in the European Alps had receded to near its present-day position. As pointed out above, the subsequent Younger Dryas snowline lowering in western Norway averaged about 450 m below today's value, compared with more than 1200 m at the LGM (Dahl and Nesje, 1992). In the European Alps, the Younger Dryas advance to the Egesen moraines, generally located 2–10 km downvalley from the Little Ice Age moraines, was accompanied by a snowline drop of about 350 m compared to the present day. Hence the Younger Dryas snowline lowering in the Alps was much less than the LGM depression of about 1200 m (Maisch, 1982, 1987, 1992).

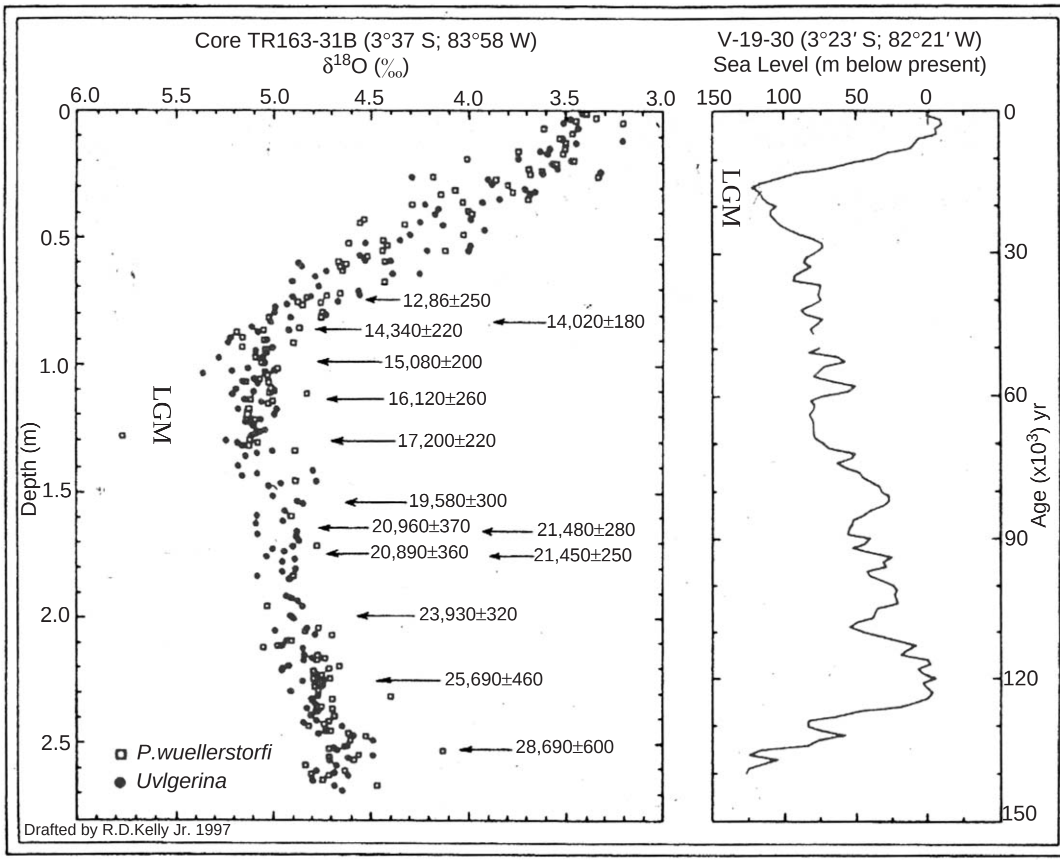

Fig. 7. The right panel, adapted from Shackleton (1987), shows a sea-level estimate based on the δ ^{18}O records of V19–30 in the equatorial eastern Pacific Ocean (3°23′S, 83°21′W) and RC-17–177 in the equatorial western Pacific Ocean (1°45′N, 159°27′E). To construct this curve, a correction for changing deep-water temperatures was made by calculating the isotopic difference between V-19–30 (benthonic) and RC 17–77 (planktonic). This difference was then subtracted from the benthonic V-19–30 record. The results were scaled to the New Guinea sea-level data to yield an estimate from isotopic data of the global sea-level record. Even though it is certainly not a perfect representation of sea level, the resulting curve nevertheless highlights the long, gradual decline of sea level (increase of continental ice volume), followed by an abrupt termination, that marked the latest 100,000-yr glacial cycle. The left panel shows the timing of the last termination in detail. The figure displays the isotope data set from equatorial eastern Pacific core TR163-31B (3°37′S, 83°58′W) from Shackleton et al. (1988), with original isotope data points kindly provided by N.J. Shackleton. The radiocarbon dates have a marine reservoir correction of 580 ^{14}C years. The results from two species of benthonic foraminifers are plotted. They are taken to be a reasonable reflection of changes in continental ice volume. They show that the fundamental change between rising and declining isotope values, which marks the beginning of the last termination, occurred close to 14,500 ^{14}C yr BP (not adjusted for unknown mixing time of the ocean at that date).

6. Other snowline and ice-core mismatches

We now turn to several older but nevertheless striking contrasts between moraine and ice-core records. We again argue that these differences reflect seasonality.

The first case involves climate signatures during and just after the LGM. The classic asymmetric shape of ice-volume (sea-level) change of the last glacial cycle is depicted in Fig. 7. Of particular importance is the prominent LGM. In the benthic oxygen-isotope record of Fig. 7, the LGM gives way to the beginning of the last termination about 14,000–14,700 ^{14}C yr BP (16,000–17,300 cal. yr BP). This turning point is a very important climate event, because it marks the change from the long declining to the short ascending limb of the last 100,000-year glacial cycle.

The timing and shape of the isotopic- and sea-level LGM in Fig. 7 corresponds with deposition of the LGM moraine belts along the southern margins of the Laurentide and Scandinavian Ice Sheets (Denton and Hughes, 1981). The beginning of the termination in the isotope record is also consistent with land-based moraine chronologies. For example, snowline rise accompanied by ice recession was underway in the Swiss Alps shortly before 14,600 ^{14}C yr BP; much of the Alps was deglaciated, and snowline had recovered at least 40% of its glacial-interglacial depression, before the abrupt Bölling transition (Schlüchter, 1998; Denton et al., 1999 and references therein). Likewise, by the beginning of the Bölling, the southern margin of the Scandinavian Ice Sheet had retreated to the Luga moraine near the Baltic Sea, considerably north of the

LGM position (Andersen, 1981; Lundquist and Saarnisto, 1995). The same situation pertained to the Laurentide Ice Sheet, which had withdrawn to the northern Great Lakes and, just before the beginning of Bölling time, stood at the Port Huron moraines well north of the LGM limit (Denton and Hughes, 1981). The southern Cordilleran Ice Sheet had already suffered considerable recession by the onset of abrupt Bölling warming (Denton and Hughes, 1981). By 12,500 ^{14}C yr BP, the complex ice lobe that extended north of the St. Elias Mountains in southern Yukon Territory at the LGM had already pulled back to the vicinity of the mountain front (Denton, 1974).

The GISP2 oxygen-isotope record from central Greenland in Fig. 2 lacks the distinct LGM shown both in Fig. 7 and in the moraine record. Instead, through much of the classic LGM marked on Fig. 2 as corresponding to the maximum ice extent defined by moraines, the oxygen-isotope ratios are no more negative than they were during the Younger Dryas or the earlier Dansgaard-Oeschger cold phases. Moreover, there is no obvious turning point at about 17,300 cal. yr BP that marks the beginning of the termination in the ice-volume and moraine proxies. This fundamental turning point is not visible even if the search interval in Fig. 2 is expanded to cover the entire time between 15,000 and 20,000 years ago to allow for mixing time of the ocean and for varying isotopic composition of the ice sheets. In fact the opposite trend occurs, because at about 17,300 cal. yr BP the oxygen-isotope ratios in the GISP2 record become more negative and persist that way until the abrupt Bölling transition (Fig. 2). In the GR1P ice-core record, this interval is referred to as Greenland stadial-2a (GS-2a in Fig. 8) (Walker et al., 1999). Thus a curious situation arises in which the moraine records suggest that the lowest summer temperatures occurred during the LGM, with rising summer temperatures heralding the beginning of the termination at about 17,300 cal. yr BP In sharp contrast the GISP2 ice core shows that mean annual temperatures during the LGM were not severely depressed. Furthermore, rather than the summer warming registered by moraines, mean annual temperature in Greenland (Fig. 2) actually declined for several thousand years during Greenland stadial-2a after the beginning of the termination illustrated in Fig. 7.

As yet another expression of this puzzle, Fig. 8 highlights the curious situation that arises when moraine records are compared with North Atlantic climate signals during Greenland stadial-2a. The top panel shows irregular sea-level rise during GS-2a. This is consistent with the aforementioned irregular recession to the Port Huron and Luga moraines, as well as collapse of alpine glaciers, by the beginning of the Bölling. In sharp contrast, mean annual temperatures in Greenland dropped during GS-2a. North Atlantic

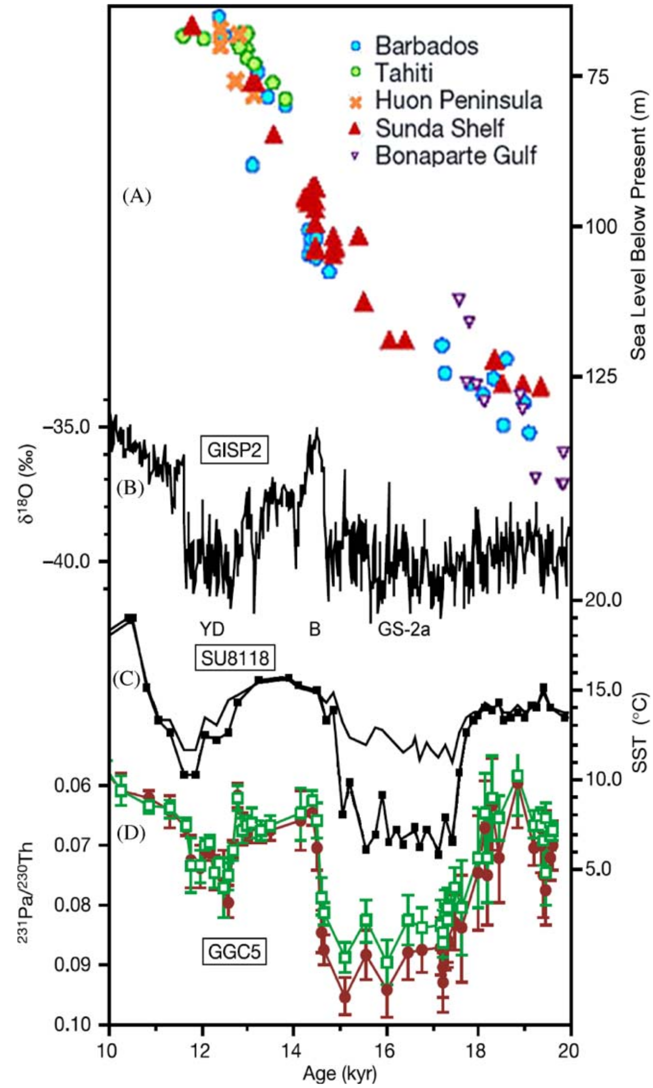

Fig. 8. North Atlantic deglacial climate signals compared with sea-level rise. A shows sea-level (Lambeck and Chappell, 2001). B shows the G1SP2 isotope record (Stuiver and Grootes, 2000). C is SST from two calibrations for alkenone unsaturation ratios (Bard et al., 2000) for core SU-8118 from off Portugal. D is a ^{231}Pa/^{230}Th profile from core GGC5 from the Bermuda Rise; this profile is a measure of the strength of Atlantic meridional overturning circulation (McManus et al., 2004). Figure adapted in part from McManus et al. (2004).

meridional overturning circulation nearly ceased (McManus et al., 2004) and subpolar SSTs declined below LGM values (Bard et al., 2002). Thus the coldest conditions in the North Atlantic, accompanied by the H-1 event (Fig. 2), occurred during GS-2a (McManus et al., 2004), not during the LGM as registered by moraines. These North Atlantic cold conditions did not come to an end until the sudden Bölling transition, by which time glaciers were already well behind their LGM positions. One way around this puzzle is to invoke seasonality. For example, LGM winters could have been only moderately depressed, perhaps because meridional overturning circulation in the North Atlantic remained relatively strong (McManus et al., 2004). But at the termination of the LGM, winter temperatures could have plunged as meridional overturning nearly ceased (Fig. 8). Thus mean annual temperatures as registered in Greenland could have declined despite the fact that modest summer warming drove coeval glacier recession and sea-level rise.

A note about North Atlantic SSTs is warranted. Using the revised analog method applied to planktonic foraminifera, Waelbroeck et al. (1998) showed approximately equivalent depression of summer and winter temperatures at the site of core SU-8118 off Portugal. A first impression is that these results contradict our suggestion of seasonality. But any such interpretation must take into account the concurrent major circulation changes in the North Atlantic illustrated in Fig. 8.

An additional case of climate-record mismatches involves the Dansgaard-Oeschger events prior to the LGM. In Fig. 2 the cold troughs of many of the Dansgaard-Oeschger oscillations approach or even exceed LGM values, particularly between 23,000 and 43,000 years ago. But snowline lowering, especially during the older part of this interval, fell well short of that of the LGM. At the inland front of the St. Elias Mountains in southern Yukon Territory, radiocarbon-dated stratigraphic sections show that glaciers did not advance northward beyond the mountain front between 29,000 and >49,000 ^{14}C yr BP (Fig. 9A) (Denton, 1974). Ice advanced far northward over the sites of these sections at the LGM. Finally, Fig. 9B illustrates the situation along the southern margin of the Laurentide Ice Sheet in the Great Lakes region. Again, the major advance was at the LGM, not earlier at the times of the Dansgaard-Oeschger cold troughs in Fig. 2. The two examples from North America are both consistent in indicating that glacial advances correlative with the Dansgaard-Oeschger stades, if they occurred at all, fell far short of the LGM moraine belts.

Another example concerning the Dansgaard-Oeschger events comes from Europe. Fig. 10 depicts pulses of ice-rafted debris from cores MD 95–2010 (located off the coast of Norway) and ENAM 93–21 (located close to the Faeroe Islands) (Elliot et al., 2001). These pulses are taken to represent climate-driven oscillations of the western margin of the Scandinavian Ice Sheet, and are correlated with the cold phases of the Dansgaard-Oeschger oscillations in Greenland ice cores. The striking feature of Fig. 10 is the extent of LGM ice rafting compared with that during the Younger Dryas pulse and during similar pulses older than 25,000 years. These relative magnitudes fit the known glacial geology. During the Younger Dryas the western margin of the Scandinavian Ice Sheet re-expanded modestly to the mid-fjord region to deposit an extensive moraine system that can be traced along the entire coastal region of Norway (Andersen, 1981). But this modest re-advance

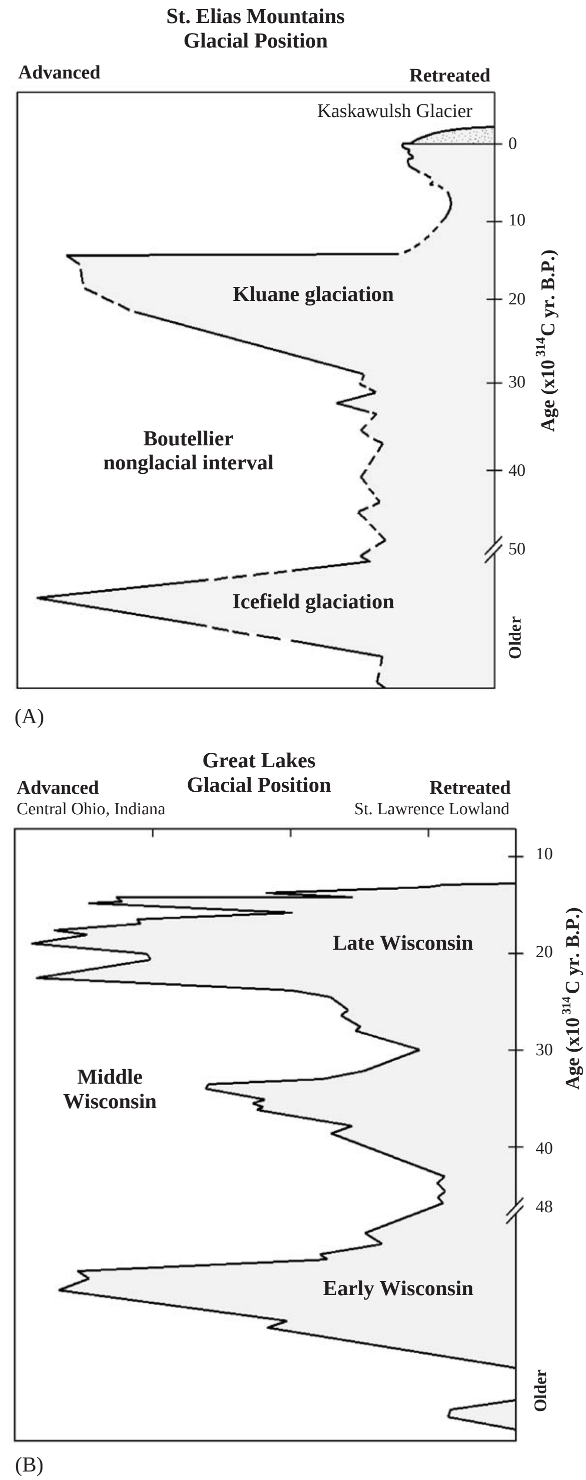

Fig. 9. (A) Time-distance diagram of glacier fluctuations along a former flow line within the glacier system that expanded northward out of the St Elias Mountains, Yukon Territory, at the LGM. The relative position of the present-day glaciers is shown by the Kaskawulsh Glacier at the top of the diagram. Adapted from Denton (1974). (B) Time-distance diagram of fluctuations of the southern margin of the Laurentide Ice Sheet during the second half of the last glacial cycle. Shown is the classic LGM in the Great Lakes region and plotted as such on Fig. 2. Adapted from Dreimanis and Goldthwait (1973).

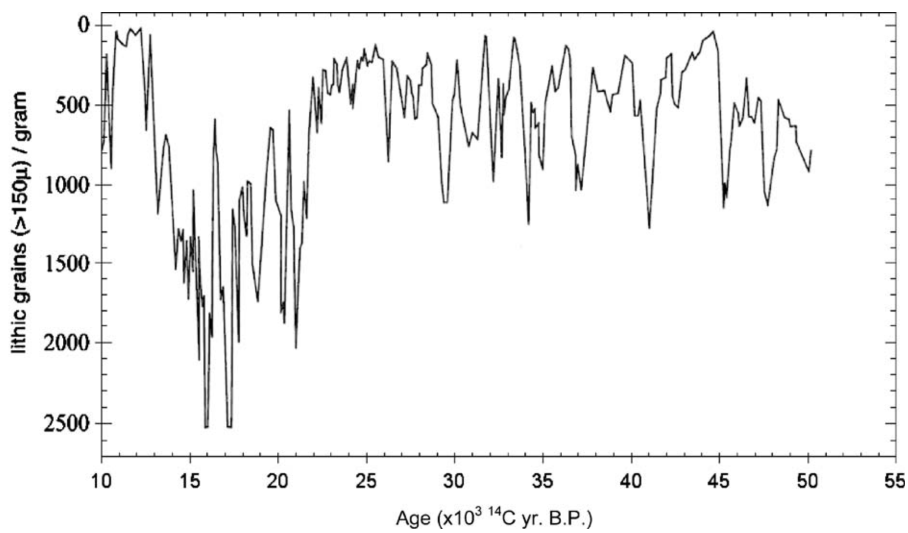

Fig. 10. A stack of ice-rafted debris records from cores MD 95-2010 (situated off the coast of Norway) and ENAM 93-21 (located close to the Faeroe Islands) in the Norwegian Sea (Elliot et al., 2001). The cores are synchronized with each other from magnetic susceptibility records. The magnetic susceptibility records so closely resemble the Greenland ice-core isotope oscillations that the position of the Greenland interstades can be transferred to the sediment record. This procedure leads to the conclusion that the pulses of ice-rafted debris between 25,000 and 50,000 ^{14}C yr BP correlate with the cold phases of Dansgaard-Oeschger events revealed in Greenland ice cores. The ice-rafting pulses are taken to represent climate-driven oscillations of the western margin of the Scandinavian Ice Sheet (Elliot et al., 2001, p. 159). This inference fits the occurrence of a pulse during the Younger Dryas, when the western margin of the Scandinavian Ice Sheet indeed re-expanded to the mid-fiord region to deposit an extensive moraine system that can be traced along the coast of Norway (Andersen, 1981). Deposition of IRD increased greatly during the LGM, a time when the western margin of the Scandinavian Ice Sheet is known to have advanced out of the fjord district onto the outer continental shelf (Andersen, 1981). Adapted from Elliot et al. (2001).

fell well short of the LGM ice-marginal position. As discussed above, the snowline lowering compared to today's value in western Norway during the Younger Dryas cold reversal was about 450 m (Fareth, 1987). Instead of during the Younger Dryas, the great increase in ice-rafted debris in Fig. 10 occurred during the LGM, when the western margin of the Scandinavian Ice Sheet is known to have advanced out of the fjord district onto the outer continental shelf (Andersen, 1981) and when snowline was 1200 m below that of today (Dahl and Nesje, 1992). In this context, the ice-rafting pulses older than the LGM and correlated with the Dansgaard-Oeschger cold troughs in Greenland are of quite modest magnitude, comparable to that of the Younger Dryas and much smaller than those of the LGM. The implication is that ice margins during the Dansgaard-Oeschger cold stadials were situated well within the LGM position, and were probably similar to that of the Younger Dryas. Again, a probable explanation for these mismatches is similar to that for the Younger Dryas. In other words, the huge mean-annual temperature declines during cold phases of the Dansgaard-Oeschger events depicted in Fig. 2 largely represent the winter season, with relatively modest summer changes.

The longer duration of the LGM compared to the stadial events allowed for closer approach of large ice masses to steady state. Hence, LGM ice sheets would have been larger than stadial ice sheets if the climates were the same. However, the millennial to multi-millennial duration of some of the stadial events, especially those associated with Heinrich events, was long enough for smaller ice masses to come close to equilibrium and for major responses of larger ice masses. Thus, we do not believe that the observations on relative glacier changes between LGM and stadials can be explained by the degree of approach to equilibrium, requiring instead that the cold of the stadials primarily reflects wintertime cooling whereas the LGM involved much summertime cooling as well.

7. Discussion

7.1. North Atlantic

To explain major mismatches between ice-core and moraine records, we have presented a case that seasonality switches dominated by wintertime were instrumental in abrupt climate changes in the North Atlantic region. The most likely source of this winter-climate leverage involves the formation of a sea-ice cover over the northern Atlantic, in response to a shutdown (or reduction in strength) of the conveyor (see Rahmstorf, 2002). By promoting the growth of sea ice, such a shutdown could have caused the entire northern tier to experience much colder winters. Sea ice was cited by Atkinson et al. (1987) to explain the remarkable switches of seasonality revealed by beetle data from the British Isles. Renssen et al. (1996), Renssen and Isarin (1998), and Isarin and Renssen (1999) also employed a North Atlantic sea-ice cover in modeling attempts to explain the enormous European seasonality flips revealed by the plant indicator species and periglacial features. And as mentioned previously, the probable seasonality switches in Greenland precipitation at Summit have been attributed to winter-time cooling and drying induced by a North Atlantic sea-ice cover (Cuffey et al., 1995; Cuffey and Clow, 1997; Fawcett et al., 1997; Jouzel et al., 1997; Krinner et al., 1997; Alley, 2000; Werner et al., 2000).

Such a spread of North Atlantic sea ice is consistent with the deep-sea-core results of McManus et al. (2004) and Dokken and Jansen (1999), which show a slowdown (or even in one case a near shutdown) of meridional overturning (and hence northward oceanic heat transport) during stades that we suggest were marked by a plunge of wintertime temperatures. And yet North Atlantic meridional overturning remained strong during the LGM (McManus et al., 2004), when we argue that depression of wintertime temperature was modest compared to that during the Younger Dryas or Dansgaard-Oeschger stades.

A remaining question is why the structure and shape of the LGM and termination was so different between the ice-core and moraine records. While we do not have an answer, perhaps the size of the ice sheets and mountain glaciers was paced by orbital cycles while the millennial events were paced by the conveyor and sea ice.

Another outstanding puzzle that we now address is whether winter-dominated seasonality switches, perhaps derived from the North Atlantic, are also embedded in the millennial-scale oscillations of the Atlantic ITCZ (Hughen et al., 1996), the Asian monsoon (Schulz et al., 1999; Wang et al., 2001; Altabet et al., 2002), and surface and intermediate-water fluctuations in the eastern North Pacific (Hendy and Kennett, 1999). We suspect that this might be the case because all of these far-field climate signals bear remarkable similarities with the ice core (winter dominated) rather than the moraine (summer dominated) records.

7.2. Atlantic intertropical convergence zone

Changes in the Atlantic ITCZ revealed in marine sediment cores of the Cariaco Basin follow the distinctive Greenland temperature signal (Fig. 11), implying that there may be a winter-dominated linkage. The trademark similarities include a weak LGM and a strong Younger Dryas signal. Chiang et al. (2003) provided a physical basis for such a connection by demonstrating in modeling experiments that fluctuations of the Atlantic ITCZ are very sensitive to North Atlantic sea-ice changes. It is thus a strong possibility that Greenland temperatures and the Atlantic ITCZ oscillate in locked step because both are linked to the spread of winter sea-ice in the North Atlantic during stadials, in turn due to a conveyor shutdown or slowdown.

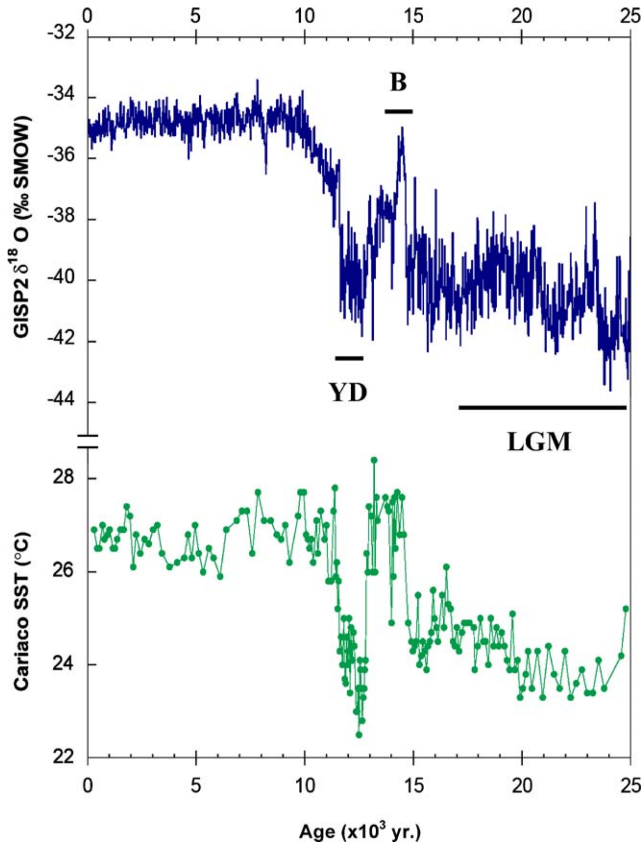

Fig. 11. Cariaco sea-surface temperatures compared with the GISP2 oxygen-isotope record. The intervals for YD, B, and LGM are the same as in Fig. 2. The chronologies for the two records are independent. Adapted from Lea et al. (2003).

7.3. Monsoon seasonality

We now turn to the Asian monsoon record. Fig. 12 gives a plot of $\delta^{15}N$ in two sediment cores from the Oman margin of the Arabian Sea near the mouth of the Persian Gulf (Altabet et al., 2002). Because of their high sedimentation rates, both cores show a record of millennial-scale variability of denitrification that mimics millennial-scale changes in the oxygen-isotope ratios of the GISP2 core in Greenland. The correspondence in the Greenland and Oman records extends not only to the number of events, but to their durations and relative magnitudes (Altabet et al., 2002). For example, both records share very strong peaks during Dansgaard-Oeschger stades, a weak LGM, declining signals right up to the abrupt Bölling transition, and a strong Younger

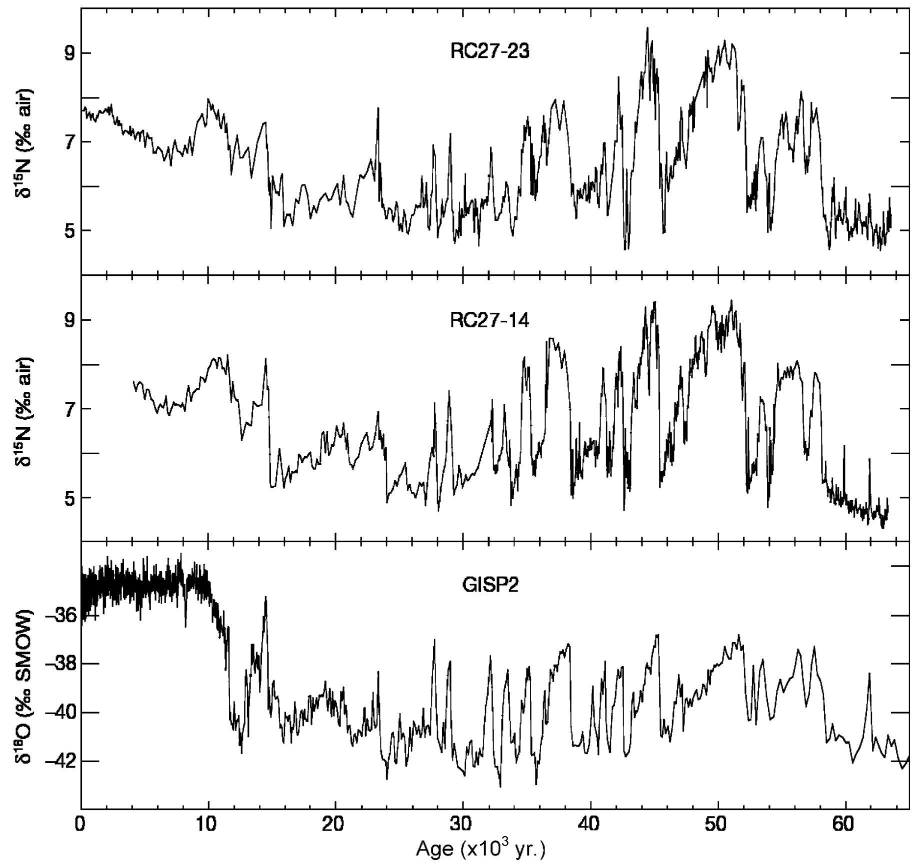

Fig. 12. High-resolution δ ^{15}N records from cores RC 27–23 and RC 27–14 from the Oman continental margin of the Arabian Sea (Altabet et al., 2002) compared with the δ^{18} O record from GISP2 in Greenland. The δ ^{15}N signal monitors denitrification, in turn related to the intensity of summer monsoonal upwelling.

Dryas. This remarkable resemblance implies a common link.

The Oman denitrification signal is tied to the intensity of summer upwelling associated with the Indian monsoon (Altabet et al., 2002). High values of summer upwelling accompany Greenland interstades, while low values match Greenland stades. Thus denitrification is at minimum values during Greenland stades and at near-modern high values during Greenland interstades. Other indicators give the same result with regard to monsoonal circulation. For example, sediment cores taken from the continental shelf of the northeastern Arabian Sea near Pakistan (Schulz et al., 1998) show a monsoonal signal nearly identical to that of the Oman cores of Altabet et al. (2002). The Pakistan continental shelf record shows weak summer monsoons coeval with cold Greenland temperatures and strong summer monsoons correlative with warm Greenland temperatures. Again, the LGM is weakly expressed but, in concert with the Greenland temperature record, the decline in summer productivity is extreme during the Dansgaard-Oeschger cold phases, as well as during the Younger Dryas. The intervals of lowest summer productivity correlate with Heinrich events in the North Atlantic, whose positions are depicted in Fig. 2. In particular, there is a plunge in productivity correlative with the North Atlantic Heinrich event 1 prior to the abrupt Bölling transition (Schulz et al., 1998).

Oxygen-isotope ratios in stalagmites from Hulu Cave in China record millennial-scale variations in the ratio of summer to winter precipitation, which in turn reflects the intensity of the East Asian summer monsoon (Wang et al., 2001), described in An (2000). The Hulu Cave signature indicates a general correspondence of weak summer monsoons during Greenland cold spells, and high summer monsoonal intensity during Greenland interstades. This is in accord with the observation from grain-size data in loess that powerful winter monsoons in China accompanied the last six Heinrich events in the North Atlantic region (Porter and An, 1995), and is consistent with the observation that Dansgaard-Oeschger stades in the North Atlantic region were accompanied by elevated concentrations and fluxes of Asian-source dust in the atmosphere above central Greenland (Alley et al., 1995; Mayewski et al., 1997; Biscaye et al., 1997).

From the nearly identical Greenland and monsoon signals, we speculate that winter-dominated seasonality was common to both regions. A potential source of winter climate leverage was highlighted more than a century ago, when Blanford (1884) suggested that winters with heavy snowfall in the western Himalayas were followed by weakening or collapse of the Indian summer monsoon, and speculated that large-scale climate changes could result from variations in the overall Eurasian snowpack. Recent observations have shown that the situation is more complex than originally envisioned by Blanford (1884), with the relation of snowfall and summer-monsoon dependent on the spatial pattern of the snow cover on the Tibetan Plateau (Zhao and Moore, 2004, and references therein).

Modeling experiments carried out by Barnett et al. (1988) show a strong tendency for late-lasting snow cover on Eurasia to weaken the subsequent summer monsoon. In the model a memory of late-lasting winter snowfall carries over well into the summer, thus slowing summer warming of the Asian land mass and reducing the land-sea temperature contrast that is a primary driver of the summer monsoon. By extension, these modeling results suggest a physical mechanism whereby long-lasting winter snow cover on the Eurasian land mass during glacial stades would link a weak Asian summer monsoon with cold Greenland and European winter temperatures.

A weak Asian summer monsoon during Greenland cold intervals could therefore have consequences for atmospheric circulation on a hemispheric scale. In the modeling results of Barnett et al. (1988), weak monsoons cause pressure and temperature changes over the Eurasian land mass, leading to downstream adjustments of the wave structure of the atmosphere and to lower-than-normal pressure over the eastern Pacific and North America. Specifically, this suggests a possible mechanism whereby monsoon-driven adjustments in the atmosphere downstream from Eurasia could have caused atmospheric reorganizations such as that called for by Hendy and Kennett (1999) to explain the stade-interstade switches revealed in sediment cores from the Santa Barbara basin on the California margin.

7.4. Overview

The millennial-scale paleoclimate signatures of the last glaciation show remarkable similarities across a huge area of the planet from Greenland to eastern Asia. These similarities include not only the number and spacing, but also the relative magnitudes of stades and interstades. Particularly prominent are the extreme stades associated with the North Atlantic Heinrich events. Such a result implies that common forcing linked the paleoclimate signal from Greenland to Asia. In this regard, all records point to seasonality switches as being important components of abrupt climate jumps. In Greenland and Europe, the switches in mean annual temperature were dominated by large winter changes. In the case of Asia, the intensity of the summer monsoon tracked Greenland temperatures, leaving cold winter monsoonal circulation prevalent during Greenland stades.

We thus speculate that winter was the common linkage between Greenland-European temperatures, the Atlantic ITCZ, and Asian monsoons. It is worth noting that when the North Atlantic is ice-covered the expanse of the Northern Hemisphere from northwest Greenland to east Asia is essentially continental and hence is susceptible to large wintertime temperature changes. This winter linkage offers an explanation as to why, in the Greenland ice cores, temperature changes are essentially synchronous with shifts of methane (summer monsoon in Asia) and dust (winter monsoon in Asia). Finally, we also speculate that, during much of the last glaciation, the climate of this huge sector of the planet was close to a critical winter threshold. Leaving aside the question of whether it originated in the atmosphere or the ocean, a perturbing trigger caused winter climate to cross this threshold repeatedly, with consequent changes in seasonality that may well have amplified and propagated the signal of abrupt climate change throughout the hemisphere and into the tropics. A key piece of the puzzle was the spread of North Atlantic sea ice as a consequence of the shutdown (or slowdown) of North Atlantic meridional overturning during cold stades.

It is clear from this discussion that a concerted effort is needed to assess the potential impacts that seasonality switches could have imposed on the Northern Hemisphere during the last ice age. One item that looms as crucial is the continental dust load in the Northern Hemisphere atmosphere (Broecker, 2001a, b, 2002). The record from GISP2 shows a ten-fold increase in dust during ice-age cold snaps (Mayewski et al., 1997). The deserts of western China seem to have been a primary source (Biscaye et al., 1997). This is precisely the region that would be affected by the switches in Asian monsoon seasonality that accompanied the Greenland temperature jumps. It is probable that persistent cold and dry winds during severe winter-dominated monsoonal circulation injected much of this Asian dust into the atmosphere. However, it should be noted that the aerosol load in the atmosphere also increased in summer, although not nearly as much as in winter (Hammer, 1997). An outstanding question is whether aerosol jumps amplified the dramatic climate swings of the Dansgaard-Oeschger, Bölling, and Younger Dryas events. It is even possible that varying summer and winter loading of atmospheric aerosols contributed to the switches in seasonality. Depending on their size and location, aerosols can reflect incoming sunlight. They can also brighten clouds by serving as condensation nuclei, thus increasing the number of droplets

(Rosenfeld, 2000). Hence, switches in aerosols could have periodically reduced the amount of sunlight reaching Earth's surface. Perhaps such a dimming effect, particularly in wintertime, helps to account for the surprisingly large amplitude of the abrupt temperature swings in the Northern Hemisphere during the last glaciation.

Acknowledgements

We thank the captain and crew of the M/V TURMOIL for their wonderful support in East Greenland: Philip Walsh, Beverly Walsh, Grant Munroe, Gerard Ellmers, Anders Spangberg, Ryan Stafford, Carolina Angel, and Christina Gomes. Telford Allen safely flew us for 10,000 km in East Greenland, for which we are very grateful. The manuscript benefited greatly from comments by George Jacobson, Svend Funder, and two reviewers. We thank Sean Brikel for help with the figures. Denton and Broecker are supported by NOAA. Alley is supported by the Office of Polar Programs of the NSF.

References

Ahlmann, H.W., 1924. Le niveau de glaciation comme fonction de l'accumulation d'humidite sous forme solide. Geografiska Annaler 3, 223–272.

Ahlmann, H.W., 1941a. The main morphological features of north-east Greenland. Geografiska Annaler 23, 148–183.

Ahlmann, H.W., 1941b. BP Studies in North-East Greenland 1939–1940, Part I, The Main morphological features of North-East Greenland. Geografiska Annaler 23, 148–152.

Ahlmann, H.W., 1941c. Studies in North-East Greenland 1939–1940, Part II, Glacial conditions in North-East Greenland in general and on Clavering Island in particular. Geografiska Annaler 23, 183–209.

Ahlmann, H.W., 1948. Glaciological research on the North Atlantic coasts. Royal Geographical Society Research Series (1), 83pp.

Ahlmann, H.W., 1953. Glacier variations and climatic fluctuations. American Geographical Society Bowman Memorial Lectures, Series 3 51pp.

Alley, R.B., 2000. The Younger Dryas interval as viewed from central Greenland. Quaternary Science Reviews 19, 213–226.

Alley, R.B., 2003. Comment on "When Earth's Freezer Door is Left Ajar". EOS 84, 315.

Alley, R.B., Koci, B.P.R., 1990. Recent warming in central Greenland? Annals of Glaciology 14, 6–8.

Alley, R.B., Finkel, R.C., Nishiizumi, K., Anandakrishnan, S., Shuman, C.A., Mershon, G.R., Zielinski, G.A., Mayewski, A., 1995. Changes in continental and sea-salt atmospheric loadings in central Greenland during the most recent deglaciation. Journal of Glaciology 41, 503–514.

Alley, R.B., Mayewski, A., Sowers, T., Stuiver, M., Taylor, K.C., Clark, 1997. Holocene climate instability: a prominent, widespread event 8200 yr ago. Geology 25, 483–486.

Alley, R.B., Brook, E.J., Anandakrishnan, S., 2002. A northern lead in the orbital band: North-south phasing of ice-age events. Quaternary Science Reviews 21, 431–441.

Altabet, M.A., Higginson, M.J., Murray, D.M., 2002. The effect of millennial-scale changes in Arabian Sea denitrification on atmospheric CO_2. Nature 415, 159–162.

An, Z., 2000. The history and variability of the East Asian paleomonsoon climate. Quaternary Sciences Reviews 19, 171–187.

Andersen, B.G., 1954. Randmorener; Sørvest-Norge. Norsk Geografisk Tidsskrift 14, 274–342.

Andersen, B.G., 1968. Glacial geology of Troms, north Norway. Norges Geologiske Undersøkelse 265 160pp.

Andersen, B.G., 1981. Late Weichselian ice sheets in Eurasia and Greenland. p1-65 and 3 plates. In: Denton, G.H., Hughes, T.J. (Eds.), The Last Great Ice Sheets. Wiley-Interscience, New York.

Anundsen, K., 1972. Glacial chronology in parts of southwestern Norway. Norges Geologiske Undersøkelse 280, 1–24.

Atkinson, T.C., Briffa, K.R., Coope, G.R., 1987. Seasonal temperatures in Britain during the past 22,000 years, reconstructed using beetle remains. Nature 325, 587–592.

Ballantyne, C.K., Harris, C., 1994. The Periglaciation of Great Britain, 330pp.

Bard, E., Rostek, F., Turon, J.-L., Gendreau, S., 2000. Hydrological impact of Heinrich events in the Northeast Atlantic. Science 289, 1321–1323.

Barnett, T., Dűmenil, L., Schlese, U., Roeckner, E., 1988. The effect of Eurasian snow cover on global climate. Science 239, 504–507.

Biscaye, E., Grousset, F.E., Revel, M., Van der Gaast, S., Zielinski, G.A., Vaars, A., Kukla, G., 1997. Asian provenance of glacial dust (stage 2) in the Greenland Ice Sheet Project 2 Ice Core, Summit, Greenland. Journal of Geophysical Research 102, 26,765–26,781.

Björck, S., Rundgren, M., Ingolfsson, O., Funder, S., 1997. The Preboreal oscillation around the Nordic Seas: terrestrial and lacustrine responses. Journal of Quaternary Sciences 12, 455–465.

Björck, S., Bennike, O., Rosén, Andresen, C., Bohncke, S., Kaas, E., Conley, D., 2002. Anomalously mild Younger Dryas summer conditions in southern Greenland. Geology 30, 427–430.

Blanford, H.F., 1884. On the connection of the Himalayan snowfall with dry winds and seasons of drought in India. Proceedings of the Royal Society of London 37, 3–22.

Bond, G., Broecker, W., Johnsen, S., McManus, J., Labeyrie, L., Jouzel, J., Bonani, G., 1993. Correlations between climate records from North Atlantic sediments and Greenland ice. Nature 365, 143–146.

Broecker, W.S., 2001a. The big climate amplifier: ocean circulation-sea ice-storminess-dustiness-albedo. American Geophysical Monograph 126, 53–56.

Broecker, W.S., 2001b. A dusty past. Preprint volume of the 12th Symposium on Global Change Climate Variations. 14–19 January 2001, Albuquerque, New Mexico by the American Meteorological Union Society. Boston, MA, pp. 175–176.

Broecker, W.S., 2002. Dust: Climate's Rusetta Stone. Proceedings of the American Philosophical Society 146, 77–80.

Broecker, W.S., Denton, G.H., 1989. The role of ocean-atmosphere reorganization in glacial cycles. Geochimica et Cosmochimica Acta 53, 2465–2501.

Brooks, S.J., Birks, H.J.B., 2001. Chironomid-inferred air temperatures from Lateglacial and Holocene sites in north-west Europe: progress and problems. Quaternary Science Reviews 20, 1723–1741.

Brooks, S.J., Mayle, F.E., Lowe, J.J., 1997. Chironomid-based Lateglacial climatic reconstruction for southeast Scotland. Journal of Quaternary Science 12, 161–167.

Chiang, J., Biasutti, M., Battisti, D.S., 2003. Sensitivity of the Atlantic Intertropical Convergence Zone to Last Glacial Maximum boundary conditions. Paleoceanography 18, 1094.

Cuffey, K.M., Clow, G.D., 1997. Temperature, accumulation, and ice sheet elevation in central Greenland through the last deglacial transition. Journal of Geophysical Research 102 c12, 26, 383-26, 396.

Cuffey, K.M., Alley, R.B., Grootes, F.M., Bolzan, J.M., Anandakrishnan, S., 1994. Calibration of the $\delta^{18}O$ isotopic paleothermometer for central Greenland, using borehole temperatures. Journal of Glaciology 40, 341–349.

Cuffey, K.M., Clow, G.D., Alley, R.B., Stuiver, M., Waddington, E.D., Saltus, R.W., 1995. Large Arctic temperature change at the Wisconsin-Holocene glacial transition. Science 270, 455–458.

Dahl, S.O., Nesje, A., 1992. Paleoclimatic implications based on equilibrium-line altitude depressions of reconstructed Younger Dryas and Holocene cirque glaciers in inner Nordfjord, western Norway. Palaeogeography, Paleoclimatology, Paleooecology 94, 87–97.

Dahl-Jensen, D., Mosegaard, K., Gundestrup, N., Clow, G.D., Johnsen, S.J., Hansen, A.W., Balling, N., 1998. Past temperatures directly from the Greenland Ice Sheet. Science 282, 268–271.

Dansgaard, W., Johnsen, S.J., Clausen, H.B., Langway Jr., C.C., 1971. Climatic record revealed by the Camp Century ice core. In: Turekian, K.K. (Ed.), The Late Cenozoic Glacial Ages. Yale University Press, New Haven, pp. 37–56.

Denton, G.H., 1974. Quaternary glaciations of the White River Valley, Alaska, with a regional synthesis for the northern St. Elias mountains, Alaska and Yukon Territory. Geological Society of America Bulletin 85, 871–892.

Denton, G.H., Hughes, T.J. (Eds.), 1981. The Last Great Ice Sheets. Wiley Interscience. New York 484pp.

Denton, G.H., Heusser, C.J., Lowell, T., Moreno, I., Andersen, B.G., Heusser, L.E., Schlüchter, C., Marchant, D.R., 1999. Interhemispheric linkage of paleoclimate during the last glaciation. Geografiska Annaler 81A, 107–153.

Dokken, T.M., Jansen, E., 1999. Rapid changes in the mechanism of ocean convection during the last glacial period. Nature 401, 458–461.

Dowdeswell, J.A., Uenzelmann-Neben, G., Whittington, R.J., Marienfield, 1994. The Late Quaternary sedimentary record in Scoresby Sund, East Greenland. Boreas 23, 294–310.

Dreimanis, A., Goldthwait, R., 1973. Wisconsinan glaciation in the Huron, Erie, and Ontario lobes. Geological Society of America Memoirs 136, 71–106.

Eicher, U., Siegenthaler, U., 1976. Palynological and oxygen isotope investigations on Late-Glacial sediment cores from Swiss lakes. Boreas 5, 109–117.

Elliot, M., Labeyrie, L., Dokken, T., Manthe, S., 2001. Coherent patterns of ice-rafted debris deposits in the Nordic regions during the last (10–60 ka). Earth and Planetary Science Letters 194, 151–163.

Fareth, O.W., 1987. Glacial geology of the middle and inner Nordfjord. Norges Geologiske Undersøkelse Bulletin 408, 1–55.

Fawcett, J., Ágústsdóttir, A.M., Alley, R.B., Shuman, C.A., 1997. The Younger Dryas termination and North Atlantic Deep Water formation: insights from climate model simulations and Greenland ice cores. Paleoceanography 12, 23–28.

Follestad, B.A., 1972. The deglaciation of the south-western part of the Folgefonn Peninsula, Hordaland. Norges Geologiske Undersøkelse 280, 31–64.

Friedrich, M., Lücke, A., Schwale, A., Hanisch, S., 2004. Late glacial environmental and climatic changes from synchronized terrestrial archives of central Europe: the network PROSIMUL. Pages News 12 (2), 27–29.

Funder, S., 1970. Notes on the glacial geology of eastern Milne Land, Scoresby Sund, East Greenland. Rap Grønlands Geol. Undersøgels 30, 37–42.

Funder, S., 1971. Observations on the Quaternary geology of the Rødefjord region, Scoresby Sund, East Greenland. Rap Grønlands Geol. Undersøgels 37, 51–55.

Funder, S., 1972a. Deglaciation of the Scoresby Sund Fjord region, north-east Greenland. Special Publication Institution of British Geogrraphy 4, 33–42.

Funder, S., 1972b. Remarks on the Quaternary geology of Jameson Land and adjacent areas, Scoresby Sund, East Greenland. Rap Grønlands Geol. Undersøgels 48, 93–98.

Funder, S., 1978. Holocene stratigraphy and vegetation history in the Scoresby Sund area, East Greenland. Grønlands Geologiska Undersøgelse Bulletin 129 66pp. and seven plates.

Funder, S., 1989. Quaternary geology of East Greenland. In: Fulton, R.J. (Ed.), Quaternary geology of Canada and Greenland. Geological Survey of Canada, Geology of Canada, pp. 743–822 no. 1 (Chapter 13).

Funder, S., 1990. Descriptive text to Quaternary map of Greenland 1:500,000, Scoresby Sund, sheet 12, 24p Copenhagen: Grønlands Geologiska Undersøgelse.

Funder, S., Hansen, L., 1996. The Greenland ice sheet–a model for its culmination and decay during and after the last glacial maximum. Meddelelser Fra Dansk Geologisk Forening 42, 137–152.

Funder, S., Hjort, C., Landvik, J.Y., 1994. The last glacial cycles in East Greenland an overview. Boreas 23, 283–294.

Funder, S., Hjort, C., Landvik, J., Nam, S.I., Reeh, N., Stein, R., 1998. History of a stable ice margin—East Greenland during the middle and upper Pleistocene. Quaternary Science Reviews 17, 77–123.

Grafenstein, U.v., Erienkeuser, H., Brauer, A., Jouzel, J., Johnsen, S., 1999. A mid-European decadal isotope-climate record from 15,500 to 5000 years BP. Science 284, 1654–1657.

Hammer, C., 1997. How rapid is a rapid climate change? Abstract in EOS 78, U12B01 F5.

Hendy, I., Kennett, J., 1999. Latest Quaternary North Pacific surface-water responses imply atmosphere-driven climate instability. Geology 27, 291–294.

Hughen, K.A., Overpeck, J.T., Peterson, L.C., Trumbore, S., 1996. Rapid climate changes in the tropical Atlantic region during the last deglaciation. Nature 380, 51–54.

Isarin, R.F.B., Bohncke, S.J., 1997. Mean July temperatures during the Younger Dryas in northwestern and central Europe as inferred from climate indicator plant species. Quaternary Research 51, 158–173.

Isarin, R.F.B., Renssen, H., 1999. Reconstructing and modeling Late Weichselian climates: the Younger Dryas in Europe as a case study. Earth Sciences Reviews 48, 1–38.

Isarin, R.F.B., Renssen, H., Koster, E.A., 1997. Surface wind climate during the Younger Dryas in Europe as inferred from aeolian records and model simulations. Palaeogeography, Palaeoclimatology, Palaeoecology 134, 127–148.

Isarin, R.F.B., Renssen, H., Vandenberghe, J., 1998. The impact of the North Atlantic Ocean on the Younger Dryas climate in northwestern and central Europe. Journal of Quaternary Science 13, 447–453.

Iversen, J., 1944. *Viscum*, *Hedera*, and *Ilex* and climate indicators. Geologiska Föreningens I Stockholm Föhandlingar 66, 463–483.

Iversen, J., 1954. The late-glacial flora of Denmark and its relation to climate and soil. Danmarks Geologiske Undersøgelse 2, 87–119.

Johnsen, S.J., Dansgaard, W., Clausen, H.B., Langway Jr., C.C., 1972. Oxygen isotope profiles through the Antarctic and Greenland ice sheets. Nature 235, 429–434.

Johnsen, S.J., Dahl-Jensen, D., Gundestrup, N., Steffensen, J., Clausen, H.B., Miller, H., Masson-Delmotte, Sveinbjörnsdottir, A.E., White, J., 2001. Oxygen isotope and paleotemperature records from six Greenland ice-core stations: Camp Century, Dye 3, GR1P, GISP2, Renland, and NorthGR1. Journal of Quaternary Sciences 16, 229–307.

Jones, R.T., Marshall, J.D., Crowley, S.F., Bedford, A., Richardson, N., Bloemendal, J., Oldfield, F., 2002. A high resolution, multi-proxy Late-glacial record of climate change and intrasystem responses in northwest England. Journal of Quaternary Science 17, 329–340.

Jouzel, J., Alley, R.B., Cuffey, K.M., Dansgaard, W., Grootes, M., Hoffman, G., Johnsen, S.J., Koster, R.D., Peel, D., Shuman, C.A., Stievenard, M., Stuiver, M., White, J.W.C., 1997. Validity of the temperature reconstruction from water isotopes in ice cores. Journal of Geopohysical Research 102, 26,471–26,487.

Kienast, M., Steinke, S., Stattegger, K., Calvert, S.E., 2001. Synchronous tropical South China Sea SST Change and Greenland warming during deglaciation. Science 291, 2132–2134.

Kobashi, T., Severinghaus, J.A., Brook, E.J., Grachev, A., 2003. Speed and magnitude of abrupt climate change at 8200 yrs BP from the Greenland ice core (GISP2)-EOS Transaction AGU 84c46, Fall meeting Supplement, Abstract, pp. 41D-04.

Krinner, G., Genthon, C., Jouzel, J., 1997. GCM analysis of local influences on ice core delta signals. Geophysical Research Letters 24, 2825–2828.

Lambeck, K., Chappell, J., 2001. Sea level change through the last glacial cycle. Science 292, 679–686.

Landais, A., Caillon, N., Severinghaus, J., Barnola, J.M., Goujon, C., Jouzel, J., Masson-Delmotte, V., 2004. Isotopic measurements of air trapped in ice to quantify temperature changes. Comptes Rendus Geoscience 336 (11), 963–970.

Larsen, E., Eide, F., Longva, O., Mangerud, J., 1984. Allerød-Younger Dryas climatic inferences from cirque glaciers and vegetational development in the Nordfjord area, western Norway. Arctic and Alpine Research 16, 137–160.

Lasca, N., 1969. The surficial geology of Skeldal, Mesters Vig, northeast Greenland. Meddelelser om Grønland, Bd 176 (3) 111pp and 3 plates.

Lea, D.W., Pak, D.K., Peterson, L.C., Hughen, K.A., 2003. Synchronicity of tropical and high-latitude Atlantic temperatures over the last glacial termination. Science 301, 1361–1364.

Liestøl, O., 1967. Storbreen glacier in Jotunheimen, Norway. Norsk Polarinstitutt Skrifter 141 63pp.

Lücke, A., Braver, A., 2004. Biogeochemical and micro-facial fingerprints of ecosystem response to rapid Late Glacial climatic changes in varied sediments of Meerfelder Maar (Germany). Palaeogeography, Palaeoclimatology, Palaeoecology 211, 139–155.

Lundquist, J., Saasnisto, M., 1995. Summary of project IGCP-253. Quaternary International 28, 9–18.

Maisch, M., 1982. Zur Gletscher-und Klimageschichte des alpinen Spätglazials. Geographica Helvetica 37, 93–104.

Maisch, M., 1987. Zur Gletschergeschichte des alpinen Spätglazials: analyse und Interpretation von Schneegrenzdaten. Geographica Helvetica 42, 63–71.

Maisch, M., 1992. Die Gletscher Graubündens. Physische Geographie 33 pp. 324–128.

Mangerud, J., Funder, S., 1994. The interglacial-glacial record at the mouth of Scoresby Sund, East Greenland. Boreas 23, 349–358.

Mayewski, A., Meeker, L.D., Whitlow, S., Twickler, M.S., Morrison, M.C., Alley, R.B., Bloomfield, P., Taylor, K., 1993. The atmosphere during the Younger Dryas. Science 261, 195–197.

Mayewski, A., Meeker, L.D., Twickler, M.S., Whitlow, S., Yang, Q., Lyons, W.B., Prentice, M., 1997. Major features and forcing of high-latitude northern hemisphere atmospheric circulation using a 110,000-year-long glaciochemical series. Journal of Geophysical Research 102, 26,345–26,366.

McDougall, D., 2001. The geomorphological impact of Loch Lomond (Younger Dryas) Stadial plateau icefields in the central Lake District, northwest England. Journal of Quaternary Science 16, 531–534.

McManus, J.F., Franciois, R., Gherardi, J.-M., Keigwin, L.D., Brown-Ledger, S., 2004. Collapse and rapid resumption of Atlantic meridional circulation linked to deglacial climate change. Nature 428, 834–837.

Nam, S., Stein, R., Grobe, H., Hubberten, H., 1995. Late Quaternary glacial-interglacial changes in sediment composition at the East Greenland continental margin and their paleoceanographic implications. Marine Geology 122, 243–262.

Oerlemans, J., 1994. Quantifying global warming from the retreat of glaciers. Science 264, 243–245.

Oerlemans, J., 2001. Glaciers and Climatic Change. A.A. Balkema Publishers, Lisse 148pp.

Paterson, W.S.B., 1994. The Physics of Glaciers, Third ed. Pergamon Press, Oxford, UK 480pp.

Porter, S.C., 1975. Equilibrium-line altitudes of late Quaternary glaciers in the Southern Alps, New Zealand. Quaternary Researchearch 5, 27–47.

Porter, S.C., An, Z.S., 1995. Correlation between climate events in the North Atlantic and China during the last glaciation. Nature 375, 305–308.

Rahmstorf, S., 2002. Ocean circulation and climate during the past 120,000 years. Nature 419, 207–214.

Renssen, H., Isarin, R.F.B.P., 1998. Surface temperature in NW Europe during the Younger Dryas: AGCM simulation compared with temperature reconstructions. Climate Dynamics 14, 33–44.

Renssen, H., Lautenschlager, M., Schuurmans, C.J.E., 1996. The atmospheric winter circulation during the Younger Dryas stadial in the Atlantic/European sector. Climate Dynamics 12, 813–824.

Rosenfeld, D., 2000. Suppression of rain and snow by urban and industrial air pollution. Science 287, 1793–1796.

Schlüchter, C., 1998. The deglaciation of the Swiss Alps: a paleoclimate event with chronological problems. Bulletin of the Association of the Francétude Quaternaire 1988-2/3, 141–145.

Schulz, H., von Rad, U., Erienkeuser, H., 1998. Correlation between Arabian Sea and Greenland climate oscillations of the past 110,000 years. Nature 393, 54–57.

Severinghaus, J., Sowers, T., Brook, E.J., Alley, R.B., Bender, M.L., 1998. Timing of abrupt climate change at the end of the Younger Dryas interval from thermally fractionated gases in polar ice. Nature 391, 141–146.

Severinghaus, J., Brook, E.J., 1999. Abrupt climate change at the end of the last glacial period inferred from trapped air in polar ice. Science 286, 930–934.

Shackleton, N.J., 1987. Oxygen-isotopes, ice volume and sea level. Quaternary Science Reviews 6, 183–190.

Shackleton, N.J., Duplessy, J.-C., Arnold, M., Maurice, P., Hall, M.H., Cartlidge, J., 1988. Radiocarbon age of last glacial Pacific deep water. Nature 335, 708–711.

Sissons, J.B., 1979a. Palaeoclimatic inferences from former glaciers in Scotland and the Lake District. Nature 278, 518–521.

Sissons, J.B., 1979b. The Loch Lomond Stadial in the British Isles. Nature 280, 199–203.

Sissons, J.B., 1980. The Loch Lomond advance in the Lake District, northern England. Transactions of the Royal Society of Edinburgh, Earth Sciences 71, 13–27.

Sissons, J.B., Sutherland, D.G., 1976. Climatic inferences from former glaciers in the south-east Grampian Highlands, Scotland. Journal of Glaciology 17, 325–346.

Steig, E.J., Grootes, M., Stuiver, M., 1994. Seasonal precipitation timing and ice core records. Science 266, 1885–1886.

Stein, R., Nam, S., Grobe, H., Hubberten, H., 1996. Late Quaternary glacial history and short-term ice-rafted debris fluctuations along the East Greenland continental margin, In Late Quaternary Paleoceanography of the North Atlantic margins. Geological Society Special Publication 111, 135–151.

Street, A.F., 1977. Deglaciation and marine paleoclimate in Schuchert Dal, Scoresby Sund, East Greenland. Arctic and Alpine Research 9, 421–426.

Stuiver, M., Grootes, M., 2000. GISP2 oxygen-isotope ratios. Quaternary Research 53, 277–284.

Sutherland, D.G., 1984. Modern glacier characteristics as a basis for inferring former climates with particular reference to the Loch Lomond Stadial. Quaternary Science Reviews 3, 291–309.

Veranger, T., Houmark-Nielsen, M., Løvberg, K., Mangerud, J., 1994. Eemian-Weichselian stratigraphy of the Flakkerhuk ridge, southern Jameson Land, East Greenland. Boreas 23, 359–384.

Waelbroeck, C., Labeyrie, L., Duplessy, J.C., Guiot, J., Labracherie, M., Leclaire, H., Duprat, J., 1998. Improving past sea surface temperature estimates based on planktonic fossil faunas. Paleoceanography 13, 272–283.

Walker, M.J.C., Björck, S., Lowe, J.J., Cwynar, L.C., Johnsen, S., Knudsen, K.-L., Wohlfarth, B., INTIMATE group, 1999. Isotopic events in the GRIP ice core: a stereotype for the Late Pleistocene. Quaternary Science Reviews 18, 1143–1150.

Wang, Y.J., Cheng, H., Edwards, R.L., An, Z.S., Wu, J.Y., Shen, C.-C., Dorale, J.A., 2001. A high-resolution absolute-dated late Pleistocene monsoon record from Hulu Cave, China. Science 294, 2345–2348.

Washburn, A.L., 1965. Geomorphic and vegetational studies in the Mesters Vig District, Northeast Greenland. Meddelelser om Grønland, bd 166 nr. 1, 60pp. and 5 plates.

Washburn, A.L., Stuiver, M., 1962. Radiocarbon-dated postglacial delevelling in Arctic north-east Greenland and its implications. Arctic 15, 66–74.

Weidick, A., 1959. Glacial variations in West Greenland in historical time. Meddelelser om Grønland 158 196pp.

Weidick, A., 1963. Ice margin features in the Julianhåb District, South Greenland. Meddelelser om Grønland 165 (3) 133pp.

Weidick, A., 1968. Observations on some Holocene glacier fluctuations in West Greenland. Meddelelser om Grønland 165 (6) 202pp.

Weidick, A., 1972. Notes on Holocene glacial events in Greenland. In: Vasari, Y., Hyvärinen, H., Hicks, S. (Eds.), Climate Change in Arctic Areas During the Last Ten-Thousand Years. Acta Uni Ouluensis A3, pp. 117–204.

Weidick, A., 1994. Historical fluctuations of calving glaciers in South and West Greenland. Rap Grønlands Geol. Unders. 161, 73–79.

Werner, M., Mikolajewicz, U., Heimann, M., Hoffmann, G., 2000. Borehole versus isotope temperatures on Greenland: seasonality does matter. Geophysical Research Letters 27 (5), 723–726.

Werner, M., Heimann, M., Hoffmann, G., 2001. Isotopic composition and origin of polar precipitation in present and glacial climate simulations. Tellus 53B, 53–71.

Zhao, H., Moore, G.W.K., 2004. On the relationship between Tibetan snow cover, the Tibetan plateau monsoon and the Indian summer monsoon. Geophysical Research Letters 31, L14204.